Localization of α-Synuclein in Teleost Central Nervous System: Immunohistochemical and Western Blot Evidence by 3D5 Monoclonal Antibody in the Common Carp, *Cyprinus carpio*

Rosa Vaccaro,[1] Mattia Toni,[2]* Arianna Casini,[1] Giorgio Vivacqua,[1] Shun Yu,[3] Loredana D'este,[1] and Carla Cioni[2]

[1]Department of Anatomical, Histological, Forensic Medicine and Orthopedics Sciences, Sapienza University, Rome, Italy
[2]Department of Biology and Biotechnology "Charles Darwin,", Sapienza University, Rome, Italy
[3]Department of Neurobiology, Beijing Institute of Geriatrics, Xuamwu Hospital, China Capital Medical University, Beijing, China

Alpha synuclein (α-syn) is a 140 amino acid vertebrate-specific protein, highly expressed in the human nervous system and abnormally accumulated in Parkinson's disease and other neurodegenerative disorders, known as synucleinopathies. The common occurrence of α-syn aggregates suggested a role for α-syn in these disorders, although its biological activity remains poorly understood. Given the high degree of sequence similarity between vertebrate α-syns, we investigated this proteins in the central nervous system (CNS) of the common carp, *Cyprinus carpio*, with the aim of comparing its anatomical and cellular distribution with that of mammalian α-syn. The distribution of α-syn was analyzed by semiquantitative western blot, immunohistochemistry, and immunofluorescence by a novel monoclonal antibody (3D5) against a fully conserved epitope between carp and human α-syn. The distribution of 3D5 immunoreactivity was also compared with that of choline acetyltransferase (ChAT), tyrosine hydroxylase (TH), and serotonin (5HT) by double immunolabelings. The results showed that a α-syn-like protein of about 17 kDa is expressed to different levels in several brain regions and in the spinal cord. Immunoreactive materials were localized in neuronal perikarya and varicose fibers but not in the nucleus. The present findings indicate that α-syn-like proteins may be expressed in a few subpopulations of catecholaminergic and serotoninergic neurons in the carp brain. However, evidence of cellular colocalization 3D5/TH or 3D5/5HT was rare. Differently, the same proteins appear to be coexpressed with ChAT by cholinergic neurons in several motor and reticular nuclei. These results sustain the functional conservation of the α-syn expression in cholinergic systems and suggest that α-syn modulates similar molecular pathways in phylogenetically distant vertebrates. J. Comp. Neurol. 523:1095–1124, 2015.

INDEXING TERMS: brain; spinal cord; ChAT (RRID:AB_2079760); TH (RRID:AB_390204); 5HT (RRID:AB_92263)

Alpha-synuclein (α-syn) is a 140 amino acid protein belonging to the synuclein family, which includes three structurally related proteins: α-, β-, and γ-syn, expressed in mammalian neurons. Structural alterations of α-syn as well as its overexpression and polymorphisms have been related to the onset and progression of several human neurodegenerative diseases, known as synucleinopathies (Spillantini et al., 1997; Martin et al., 2006; Al-Chalabi et al., 2009; Scholz et al., 2009). Pathological, biochemical, and genetic evidence suggest a crucial role for α-syn in the pathogenesis of Parkinson's disease (PD) (Kanaan and Manfredsson, 2012). Indeed, α-syn aggregates are the main component of the established pathologic hallmarks of PD, the Lewy bodies and Lewy neurites (Spillantini et al., 1997; Vilar et al., 2008). Cellular inclusions of α-syn are also the key pathological features of dementia with Lewy

Grant sponsor: Sapienza University of Rome (progetti di ricerca 2012).

*CORRESPONDENCE TO: Mattia Toni, Via Alfonso Borelli 50, 00161 Rome, Italy. E-mail: mattia.toni@uniroma1.it

Received June 13, 2014; Revised December 3, 2014;
Accepted December 3, 2014.
DOI 10.1002/cne.23722
Published online February 17, 2015 in Wiley Online Library (wileyonlinelibrary.com)

bodies (Okazaki et al., 1961) and Multiple System Atrophy, with different topographical and cellular distribution in both neurons and glial cells. The common occurrence of α-syn aggregates suggests a shared pathological mechanism for these neurodegenerative disorders, although the biological activity of α-syn and its precise role in neurodegeneration remain poorly understood. Based on these assumptions, understanding the biological functions of α-syn appears to be an important approach to elucidate the pathogenesis of such diseases and to facilitate the identification of new therapeutic targets for synucleinopathies.

Alpha-syn was first cloned and isolated from the electric organ of *Torpedo californica* (Carlson and Kelly, 1980). Afterwards, Maroteaux et al. (1988) demonstrated that the syn gene is specifically expressed in electromotoneurons where the protein is localized at the presynaptic nerve terminals and at the nuclear envelope. These authors suggested that syn proteins are involved in the coordination of nuclear and synaptic events and also demonstrated that the syn gene is not expressed at the same levels in all regions of the central nervous system (CNS). A gene homologous to *Torpedo* syn was then recognized in the rat brain and the encoded protein was named α-syn. Afterwards, additional β- and γ-syn were identified in mammals. It was shown that three different genes encode the three proteins and the existence of additional syn members was interpreted as a compensatory mechanism against the loss of α-syn gene or protein (Chandra et al., 2004; Robertson et al., 2004; Burré et al., 2010; Greten-Harrison et al., 2010).

Biochemical studies in mammals showed that α-syn interacts with cytoskeletal proteins (Sharma et al., 2001; Alim et al., 2004), neuronal receptors (Cheng et al., 2011), presynaptic proteins (Burré et al., 2010), and enzymes involved in histones acetylation (Goers et al., 2003) to modulate their functions (Jenco et al., 1998; Neystat et al., 2002). Other evidence suggested that α-syn is involved in synaptic integrity and that the loss of its biological function seriously impaired neuronal function (Jellinger, 2011).

Immunohistochemical studies demonstrated that α-, β-, and γ-syn are differentially distributed in the CNS of mammals and the observed differences were related to functional differences among the three proteins (Li et al., 2002; Adjou et al., 2007; Ubeda-Banon et al., 2010). Indeed, α-syn is predominantly associated with the catecholaminergic systems, whereas β-syn is typically weak or absent in catecholaminergic neurons, being mainly localized in somatic cholinergic neurons. γ-syn was instead reported in both cholinergic and catecholaminergic regions. A functional relationship between α-syn and dopaminergic neurotransmission was suggested by evidence demonstrating that α-syn regulates the synthesis, storage, release, and reuptake of dopamine (Perez et al., 2002; Yu et al., 2005).

The three syns have been localized in different intracellular compartments of mammalian neurons. Thus, α- and β-syn are preferentially located in presynaptic terminals, whereas γ-syn is also abundant in the neuronal perikarya (Li et al., 2002; Totterdel et al., 2004; Yamada et al., 2004). In presynaptic terminals, α-syn is associated with synaptic vesicles and presumably involved in synaptic transmission and vesicle recycling (Cheng et al., 2011). The nuclear localization of α-syn in mammalian neurons appeared controversial until two novel monoclonal antibodies, 2E3 and 3D5, were developed against different epitopes of human α-syn (Yu et al., 2007) that were able to discriminate the presynaptic from the nuclear α-syn. Indeed, 2E3 antibody detects α-syn in the nerve fibers, whereas 3D5 preferentially detects α-syn in the neuronal nuclei. Both antibodies are able to detect α-syn at presynaptic terminals. By using these antibodies, it was shown that the expression of α-syn is ubiquitous in the CNS of mammals, although its cellular localization differs markedly in the various regions (Zhang et al., 2008; Vivacqua et al., 2009, 2011a,b). These results suggested that α-syn plays different roles, probably by interacting with specific intracellular proteins and modulating the physiological activity of different neurons.

Since Maroteaux et al.'s (1988) pioneering work on the electric ray, some data were added on the evolutionary and functional conservation of synucleins. These appear to be vertebrate-specific proteins, with no counterparts found in invertebrates, such as *Caenorhabditis elegans*, *Drosophila melanogaster*, or *Ciona intestinalis* (Hamilton, 2004). The α-syn coding mRNA was sequenced in representative species of all vertebrates and the comparison of the deduced amino acid sequences demonstrated that α-syn is evolutionarily conserved (Tiunova et al., 2000; Yoshida et al., 2006; Larsen et al., 2009). Nonetheless, the anatomical and cellular distribution of α-syn is little known in nonmammalian vertebrates (Martinez-Navarrete et al., 2007). Given the high degree of α-syn sequence conservation, the biological properties of this protein may be investigated in nonmammalian vertebrates. The usefulness of fish models to study pathogenic mechanisms that lead to synucleinopathies was recently stressed by Boudreau et al. (2009), who showed the increase in α-syn-like immunoreactivity after metal ion exposure, leading to potential CNS toxicity, in *Catostomus commersoni*. Moreover, a genetic and toxin-induced fish model was recently generated for PD by medaka, *Oryzias latipes* (Matsui et al., 2009, 2010).

The aim of the present study was to analyze the anatomical and cellular distributions of α-syn in the CNS of the cyprinid teleost, *Cyprinus carpio*. Among cyprinids, the zebrafish has been established as the fish model for neurodegenerative diseases (Phillips et al., 2009; Panula et al., 2010), given that human genes implicated in several neurological disorders have their evolutionary orthologs in this species (Flinn et al., 2008; Willemsen et al., 2008; Sager et al., 2010). However, zebrafish lacks the α-syn (*snca*) gene (Sun and Gitler, 2008; Chen et al., 2009; Milanese et al., 2012), having three syn genes, *sncb, sncg1*, and *sncg2* (encoding β-, γ1-, and γ2-syn, respectively), highly conserved with respect to their human paralogs. Given this peculiar condition in zebrafish, a preliminary search was made in protein databases to identify all the available α-syn sequences from teleosts. Sequence comparisons showed that α-syn partial amino acid sequences from both *C. carpio* (Larsen et al., 2009) and *Silurus glanis* share the highest percent homology with human α-syn. Therefore, the common carp, which is a close relative of zebrafish, was chosen as the model species for the present analysis. In this study, regional expression of α-syn was first analyzed in the CNS by semiquantitative western blot (WB) performed with a commercial polyclonal anti-α-syn or with the monoclonal 3D5 antibody (Yu et al., 2007), which recognizes fully conserved epitopes between carp and human proteins. The anatomical and cellular α-syn distribution was then mapped by 3D5 immunohistochemistry in the CNS with the aim of identifying both nuclear and presynaptic α-syn. In addition, α-syn-positive neurons of the carp were neurochemically characterized by choline acetyltransferase (ChAT), tyrosine hydroxylase (TH), and serotonin (5HT) single and double immunohistochemistry. The results presented here provide the first detailed description of α-syn expression in the CNS of teleosts.

MATERIALS AND METHODS

Animals and sampling

Four adult individuals of *Cyprinus carpio* (Taxon 7962) (*s.l.9 cm)*, obtained by local authorized providers, were anesthetized by adding 2phenoxyethanol to the fish tank (final concentration of 1.5 ml/l) and successively transcardially perfused by PFA fixative (4% paraformaldehyde in 0.1M phosphate buffer), pH 7 at 4°C. The brains were quickly removed from the skulls and postfixed in the same fixative for 24 hours, then stored at 4°C in 0.01 M phosphate buffer (PB) containing 15% of sucrose. Samples were frozen and cut on a cryostat (HM 505 E, Microm, Germany) into 30-μm-thick coronal serial sections that were stored until use in 24-well plates containing cold 15% sucrose PB, each well containing a single section to allow the sections to thaw and float in the buffer; sections were enumerated to avoid misplacement, maintaining the seriality. Before immunohistochemical staining, the free-floating sections were treated with 0.01 M phosphate-buffered saline (PBS) containing 0.3% Triton X-100 (PBST) at 4°C for 2 or 3 days, to improve tissue permeability.

All experiments were performed in accordance with the Directive 2010/63/EU (EU 2010) and were approved by the Italian administrative order DM 70/96 of Italian Ministry of Health.

Sequence analysis

The amino acid sequences of teleost synucleins were sought in the NCBI protein database (http://www.ncbi.nlm.nih.gov/protein, RRID:nif-0000–03178). Both the deduced and predicted amino acid sequences were considered. A total of 39 sequences defined by different Accession Numbers were detected (Table 1). The comparative analysis of the amino acid sequences was performed with ClustalW2 software (http://www.ebi.ac.uk/Tools/msa/clustalw2/, RRID:nif-0000–30076).

Antibodies

Three different antibodies against the C-terminus of human α-syn were first compared to evaluate their putative ability to recognize carp α-syn: two noncommercial mouse monoclonal antibodies (3D5, Department of Neurobiology, Xuanwu Hospital, Capital Medical University Cat. no. 3D5 mouse antihuman α-synuclein antibody, RRID:AB_2315787 and 2E3, Department of Neurobiology, Xuanwu Hospital, Capital Medical University Cat. no. 2E3 mouse monoclonal antihuman α-synuclein antibody, RRID:AB_2315791) directed respectively against the epitopes DMPVDPD (115–121 in human α-syn) and QDYEP (amino acids 134–138 in human α-syn) (Yu et al., 2007), and a commercial rabbit polyclonal antibody against the 111–131 region of human α-syn (Millipore, Bedford, MA; Cat. no. AB5038, RRID:AB_91648) (see Results for details). On the basis of the comparison between human and teleost α-syn amino acid sequences, two of them, 3D5 monoclonal and the polyclonal antibody, were chosen for western blot and immunohistochemical analyses. Moreover, a commercial β-actin antibody (Santa Cruz Biotechnology, Santa Cruz, CA; Cat. no. sc-47778, RRID:AB_626632) was used to normalize western blot results. Moreover, commercial polyclonal antibodies against ChAT, TH, and 5HT were used for immunohistochemistry and immunofluorescence.

The anti-ChAT polyclonal antibody (EMD Millipore, Cat. no. AB143, RRID:AB_2079760) was produced against human placental enzyme and it has been tested

Abbreviations

A	anterior thalamic nucleus
ac	anterior commissure
acd	anterior commissure, dorsal part
acv	anterior commissure, ventral part
Br	brainstem
cc	central canal
CCe	cerebellar corpus
Ce	cerebellum
Cgus	commissure of the secondary gustatory nucleus
CM	mammillary body
CO	optic chiasm
CP	central posterior thalamic nucleus
Ctec	tectal commissure
dDl	dorsal region of Dl
DH	dorsal horn
Di	diencephalon
DiV	diencephalic ventricle
Dl	lateral zone of dorsal telencephalic area
Dm	medial zone of dorsal telencephalic area
DMLX	lateral column of the vagal motor complex
fr	habenulo-interpeduncular tract
ggl	ganglionic layer of cerebellum
gran	granular layer of cerebellum
hc	horizontal commissure
Hc	caudal hypothalamus
Hd	dorsal zone of periventricular hypothalamus
Hv	ventral zone of periventricular hypothalamus
IG	intermediate gray, spinal cord
IL	inferior lobe of hypothalamus
IMRF	intermediate reticular formation
IR	inferior raphe
IRF	inferior reticular formation
LC	locus coeruleus
llf	lateral longitudinal fascicle
LR	lateral recess of diencephalic ventricle
Ma	Mauthner axon
mlf	medial longitudinal fascicle
mol	molecular layer of cerebellum
MON	medial octavolateralis nucleus
NAT	anterior tuberal nucleus
NCLI	central nucleus of inferior lobes
NI	isthmic nucleus
nIII	oculomotor nucleus
nIIIsd	oculomotor nucleus , dorsal subdivision
NIn	interpeduncular nucleus
nIV	trochlear nucleus
NLT	lateral tuberal nucleus
Nmlf	nucleus of the medial longitudinal fascicle
nVIIm	facial motor nucleus
nVm	trigeminal motor nucleus
nVmd	trigeminal motor nucleus, dorsal subdivision
nXm	vagal motor nucleus
OT	midbrain tectum
pc	posterior commissure
PGm	medial preglomerular nucleus
PGZ	periventricular gray zone of optic tectum
PPa	parvocellular preoptic nucleus, anterior part
PPd	periventricular pretectal nucleus, dorsal part
PPp	parvocellular preoptic nucleus, posterior part
PPv	periventricular pretectal nucleus, ventral part
PTN	posterior tuberal nucleus
R	rat brain homogenate
rpo	preoptic recessus
RTN	rostral tegmental nucleus
RV	rhombencephalic ventricle
SC	spinal cord
SCN	suprachiasmatic nucleus
SG	subglomerular nucleus
SGN	secondary gustatory nucleus
SR	superior raphe
SRF	superior reticular formation
SRN	superior reticular nucleus
T	telencephalon
TL	longitudinal torus
TPp	periventricular nucleus of posterior tuberculum
TS	semicircular torus
ttb	tecto-bulbar tract
ttbc	crossed tecto-bulbar tract
Va	valvula cerebelli
Vd	dorsal nucleus of ventral telencephalic area
vDl	ventral region of Dl
VH	ventral horn, spinal cord
VL	ventrolateral thalamic nucleus
Vl	lateral nucleus of ventral telencephalic area
VM	ventromedial thalamic nucleus
Vv	ventral nucleus of ventral telencephalic area
XL	vagal lobe

in human, mouse, rat, monkey, bat, and feline, showing crossreactivity among these species (manufacturer's technical information). The anti-ChAT antibody has been previously used in confocal microscopy analysis on *Electrophorus electricus* (Nunes-Tavares et al., 2000).

The anti-TH rabbit polyclonal antibody (EMD Millipore, Cat. no. AB152, RRID:AB_390204) was produced against TH from rat pheochromocytoma denatured by sodium dodecyl sulfate (SDS). The anti-TH antibody in western blot selectively labeled a single band at ~62 kDa corresponding to TH. The antibody reactivity has been tested in rat, mouse, ferret, feline, and *Aplysia californica* (marine mollusc) (manufacturer's technical information). The same antibody has been previously used to stain TH in the goldfish (Morita and Finger, 1987; Hornby and Piekut, 1990), the stickleback (Ekström et al., 1990), the mormyrid (Meek et al.,1993), the filefish (Funakoshi et al., 2002), the zebrafish (Bricaud et al., 2001; Yamamoto et al., 2011), the cichlid fish *Astatotilapia burtoni* (O'Connell et al., 2013), and the Japanese eel *Anguilla japonica* (Mukuda et al., 2005). Moreover, recently the same antibody has been tested by western blot and immunofluorescence in the Indian major carp, *Cirrhinus cirrhosus* (Kumar et al., 2014).

The rabbit polyclonal anti-5HT antibody (EMD Millipore, Cat. no. AB938, RRID:AB_92263) has been produced against serotonin covalently bound to bovine thyroglobulin with carbodiimide and it has been evaluated for its ability to stain serotonin-containing structures in the human ileum (manufacturer's technical information). The anti-5HT antibody has been previously successfully used in immunohistochemical studies in the Scottish powan *Coregonus lavaretus* (*L*.) (Dezfuli et al., 2005) and in brown trout *Salmo trutta* (*L*.) (Dezfuli et al., 2008).

Western blot

Two specimens were anesthetized and euthanized by an overdose of 2phenoxyethanol (8 ml/L) and the brain and spinal cord were quickly dissected out at the binocular microscope. Brains were then subdivided by iridectomy scissors into the following samples, including the main brain regions: telencephalon, diencephalon, midbrain tectum, cerebellum, and brainstem (including medulla oblongata and midbrain tegmentum). Samples were homogenized in a denaturing lysis buffer containing

TABLE 1.

Amino Acid Sequences of Teleost Synucleins Available at the NCBI Protein Database (www.ncbi.nlm.nih.gov/protein)

			Species	Accession number
Teleost	Alpha syn.	1	*Cyprinus carpio**	ACS68572.1
		2	*Esox lucius*	ACO14186.1
		3	*Astatotilapia burtoni*	XP_005931264.1
		4	*Maylandia zebra*	XP_004549660.1
		5	*Oreochromis niloticus*	XP_003455005.1
		6	*Oryzias latipes*	XP_004080506.1
		7	*Pundamilia nyererei*	XP_005720462.1
		8	*Silurus glanis* *	ACS68574.1
		9	*Takifugu rubripes*	NP_001029020.1
		10	*Xiphophorus maculatus*	XP_005812724.1
	Beta syn.	1	*Anoplopoma fimbria*	ACQ58608.1
		2	*Danio rerio*	AAI63140.1 NP_957263.1 ACA96673.1 AAH55608.1
		3	*Astatotilapia burtoni*	XP_005916463.1 XP_005916464.1
		4	*Maylandia zebra*	XP_004541135.1
		5	*Oreochromis niloticus*	XP_003445901.1
		6	*Oryzias latipes*	XP_004073444.1 XP_004073445.1 XP_004073446.1
		7	*Osmerus mordax*	ACO09057.1
		8	*Pundamilia nyererei*	XP_005719687.1
		9	*Salmo salar* 1	NP_001135131.1 ACI68037.1
		10	*Salmo salar* 2	AGH92511.1 ACM08255.1
		11	*Salmo salar* 3	ACM08337.1
		12	*Takifugu rubripes*	NP_001029018.1 ABA10448.1
		13	*Xiphophorus maculates*	XP_005795466.1 XP_005795467.1
	Gamma syn.	1	*Danio rerio 1a*	ACA96674.1
		2	*Danio rerio 1b*	ACA96675.1
		3	*Oryzias latipes* 1	XP_004077051.1
		4	*Oryzias* latipes 2	XP_004077052.1
		5	*Takifugu rubripes* 1	NP_001029017.1
		6	*Takifugu rubripes* 2	NP_001029019.1
Human	α	1	*Homo sapiens*	P37840.1
	β	2		NP_001001502.1
	γ	3		NP_003078.2

The accession numbers of the sequences are reported. Asterisks indicate the partial sequences.

urea (8M urea, 50 mM Tris-HCl, pH 7.6, 0.1M 2-mercaptoethanol, 1 mM dithiothreithol [DTT], 1 mM phenylmethylsulphonyl fluoride) and protease inhibitors (Roche, Germany) and the particulate matter was removed by centrifugation at 14,000*g* for 20 minutes. The protein concentration was determined by the Lowry method (1951). For gel electrophoresis, proteins were denatured after boiling in Laemmli Sample Buffer for 5 minutes. Then 50 μg of proteins was loaded in each lane and separated in 15% SDS-polyacrylamide gels (SDS-PAGE) according to Laemmli (1970). After electrophoresis, gels were transferred to nitrocellulose paper (Hybond C+ Extra, GE Healthcare, UK). Membranes were stained with Ponceau S to confirm the transfer of proteins. In preliminary tests, three different saturation buffer were tested: 5% nonfat milk powder in TBS-Tween, Amersham ECL Prime Blocking Agent (GE Healthcare, UK), and 5% bovine serum albumin in TBS-Tween. The last buffer allowed better results and was used in the subsequent analysis. The α-syn detection was achieved with the 3D5 mouse monoclonal antibody diluted at 1:500 or with a rabbit α-syn polyclonal antibody (α-syn pol) diluted at 1:2,000 (Millipore, Temecula, CA) and then with the appropriate peroxidase-conjugated secondary antibodies diluted at 1:5,000 (Sigma-Aldrich, St. Louis, MO; Cat. no. A9044, RRID:AB_258431 and Sigma-Aldrich Cat. no. A9169, RRID:AB_258434). Normalization was made against β-actin expression diluted at 1:3,000 (Santa Cruz Biotechnology, Dallas, TX). Rat brain homogenates were used as positive controls and negative controls were performed by the omission of primary antibodies. Detection was done using the Westar ηC Ultra enhanced chemiluminescent HRP substrate (Cyanagen, Italy) and Kodak X-Omat LS films (Sigma-Aldrich). The developed films were scanned as tiff images in eight-bit gray scale format at a setting of 300 dpi and the band intensities were measured by ImageJ software (National Institutes of Health, Bethesda, MD). In electrophoresis experiments, the "Amersham Full-Range Rainbow Molecular Weight Markers (12–225 KDa)" were used.

Immunohistochemistry (IHC) and immunofluorescence (IF)

Single IHC

In order to inactivate the endogenous peroxidase activity, the sections were pretreated for 1 hour at room temperature with PBST containing 0.1% sodium azide and 0.5% H_2O_2. To avoid the aspecific antibody binding, sections were preincubated with normal horse (goat, for polyclonal primary antibodies) serum (Vector Laboratories, Burlingame, CA) diluted 1:50 in PBST containing 1% bovine serum albumin (BSA, Sigma). Free-floating sections were then incubated for 5 days at 4°C with monoclonal 3D5 (1:3,000), or α-syn pol (1:60,000), ChAT (1:5,000), TH (1:5,000), 5HT (1:10,000). Sections were then incubated for 1 hour at room temperature with biotinylated horse antimouse immunoglobulin (Vector Laboratories, Cat. no. BA2000, RRID:AB_2313581) or biotinylated goat antirabbit

immunoglobulin (Vector Laboratories, Cat. no. BA-1000, RRID:AB_2313606) for polyclonal primary antibodies diluted 1:1,000 with PBST/BSA and then incubated for 45 minutes at room temperature with avidin-biotin-peroxidase complex (ABC, Elite Kit; Vector Laboratories) diluted 1:2,000 with PBST. The peroxidase activity was evidenced by a reaction with a solution containing 0.04% of 3,3′-diaminobenzidine-tetrahydrochloride (DAB, Fluka, Buchs, Switzerland), 0.4% of nickel ammonium sulfate, and 0.003% of H_2O_2 in 0.5 M Tris-HCl buffer, pH 7.6 for 3 minutes at room temperature. The stained sections were mounted on glass slides maintaining the seriality, dehydrated, cleared, and coverslipped with Permount (Fisher Scientific, Pittsburgh, PA).

Double IHC/IF

Selected sections were processed by double immunoperoxidase or immunofluorescent labeling.

Double IHC

Sections immunolabeled for 3D5 with the DAB method, incubated with polyclonal anti ChAT (1:5,000), TH (1:5,000) or 5HT (1:10,000), and the last immunoperoxidase activity was revealed by a 5-minute reaction with Novared solution (Novared substrate kit, Vector Laboratories).

Double IF

Sections were incubated with the following paired primary antibodies: 3D5 (1:2,000) + anti-ChAT (1:3,000) for 5 days at 4°C. Incubation with primary antibodies was followed by a 1-hour incubation with biotinylated horse antimouse IgG (1:1,000). Sections were then incubated for 1 hour at room temperature with a mixture of Cy2-conjugated streptavidin (green 1:1,000, Jackson ImmunoResearch, West Grove, PA; Cat. no. 016–220-084, RRID:AB_2307356) and Cy3-conjugated goat antirabbit IgG (red 1:400, Jackson ImmunoResearch, Cat. no. 711-165-152, RRID:AB_2307443). After several washes with PBS the sections were mounted on slides, coverslipped with PBS containing 50% of glycerol and observed under a fluorescence microscope (AX70 Provis, Olympus Optical, Japan).

Controls

For specificity controls the primary antiserum was substituted with PB alone or with suitably diluted normal serum. Preadsorption test: α-syn pol and 3D5 antiserum were preincubated with 25 mg/ml of human recombinant α-syn for 24 hours at 4°C before applying the anti-α-syn antibodies for immunostaining on tissue sections.

Image acquisition and processing

Photomicrographs were captured using an AX70 Provis microscope (Olympus Optical). Images were captured using a cooled CCD digital camera (Spot, Diagnostic Instruments, Sterling Heights, MI) and the IAS 2000 software (Delta Sistemi, Rome, Italy) and saved as tiff files. Images were digitally processed in Adobe Photoshop CS5 (San Jose, CA). Only general contrast adaptations were made, and figures were not otherwise manipulated. The schematic drawings of transverse sections through the carp brain were made by tracing digital photographic images using Corel Draw 11 software (Ottawa, Canada). The final figure composition was done using Microsoft Office Powerpoint 2008 software (Redmond, WA).

RESULTS

Sequence comparison of teleost synucleins

In the NCBI protein database 39 amino acid sequences of teleost synucleins, deduced or predicted from nucleotide sequences, were available. These sequences correspond to 29 different amino acid sequences (see Table 1 for details). For α-syn, eight complete (*Esox lucius*, *Haplochromis (=Astatotilapia) burtoni*, *Maylandia zebra*, *Oreochromis niloticus*, *Oryzias latipes*, *Pundamilia nyererei*, *Takifugu rubripes*, *Xiphophorus maculatus*,) and two partial (*Cyprinus carpio*, *Silurus glanis*) amino acid sequences were found. For β-syn, 23 sequences corresponding to 13 different and complete amino acid sequences were available: *Anoplopoma fimbria*, *Danio rerio*, *Astatotilapia burtoni*, *Maylandia zebra*, *Oreochromis niloticus*, *Oryzias latipes*, *Osmerus mordax*, *Pundamilia nyererei*, *Salmo salar* (three different amino acid sequences), *Takifugu rubripes*, *Xiphophorus maculatus*. For γ synucleins, six different amino acid sequences were known: *Danio rerio* 1a and 1b, *Oryzias latipes* 1 and 2, *Takifugu rubripes* 1 and 2.

The comparative analysis between human and teleost synucleins showed a high variability, with a percentage of homology ranging from 32 to 99% (Table 2). The highest homology was detected between human α-syn and the partial sequences of α-syn from *Cyprinus carpio* and *Silurus glanis*. The two sequences from *C. carpio* and *S. glanis* are identical (Fig. 1A) and correspond to the residues 5–129 of the human isoform (Fig. 1A). It is not known whether the unsequenced C-terminal region of the carp α-syn is also homologous to the human one. The percentage of homology among teleost α-syns ranges from 48 (*O. latipes/E. lucius and O. latipes/T. rubripes*) to 100% (*A. burtoni*, *M. zebra, P. nyererei*) and the sequence alignment showed a higher homology in the N-terminal region than in the C-terminal region of the protein (Table 2, Fig. 1B). The seven degenerate 11-residue repeats which in human α-syn form the amphipathic α-helix involved in membrane binding (Davidson

TABLE 2.

Determination of the Percentage Identity of Human and Teleost Synucleins Amino Acid Sequences, Using the ClustalW2 software at www.ebi.ac.uk/Tools/msa/clustalw2/

		Alpha syn.										Beta syn.										Gamma syn.							
		C. carpio	*E. lucius*	*A. burtoni*	*M. zebra*	*O. niloticus*	*O. latipes*	*P. nyererei*	*S. glanis*	*T. rubripes*	*X. maculatus*	*A. fimbria*	*D. rerio*	*A. burtoni*	*M. zebra*	*O. niloticus*	*O. latipes*	*O. mordax*	*P. nyererei*	*S. salar 1*	*S. salar 2*	*S. salar 3*	*T. rubripes*	*X. maculatus*	*D. rerio* 1a	*D. rerio* 1b	*O. latipes 1*	*O. latipes 2*	*T. rubripes 1*	*T. rubripes 2*	*H. sapiens* α	*H. sapiens* β
Alpha syn.	*E. lucius*	58																														
	A. burtoni	58	79																													
	M. zebra	58	79	100																												
	O. niloticus	58	78	99	99																											
	O. latipes	53	48	50	50	50																										
	P. nyererei	58	79	100	100	99	50																									
	S. glanis	100	58	58	58	58	53	58																								
	T. rubripes	60	71	84	84	83	48	84	60																							
	X. maculates	59	80	87	87	87	50	87	59	80																						
Beta syn.	*A. fimbria*	38	45	44	44	44	42	44	38	44	45																					
	D. rerio	54	44	48	48	47	44	48	54	46	49	79																				
	A. burtoni	44	42	46	46	46	38	46	44	46	47	96	83																			
	M. zebra	44	42	46	46	46	38	46	44	46	47	96	83	100																		
	O. niloticus	44	42	46	46	46	38	46	44	46	47	96	83	100	100																	
	O. latipes	45	47	44	44	44	42	44	45	45	46	93	81	94	94	94																
	O. mordax	43	45	45	45	44	36	45	43	46	42	85	84	86	86	86	85															
	P. nyererei	44	42	46	46	46	38	46	44	46	47	96	83	100	100	100	94	86														
	S. salar 1	40	42	42	42	42	36	42	40	42	38	76	65	75	75	75	75	73	75													
	S. salar 2	39	42	42	42	42	34	42	39	43	38	75	64	74	74	74	75	72	74	95												
	S. salar 3	33	41	41	41	41	36	41	33	44	38	68	65	67	67	67	67	77	67	100	90											
	T. rubripes	44	42	45	45	45	36	45	44	45	45	94	83	97	97	97	94	89	97	76	75	68										
	X. maculates	44	41	46	46	46	35	46	44	46	47	93	81	97	97	97	93	88	97	76	75	68	97									
Gamma syn.	*D. rerio* 1a	52	51	47	47	48	75	47	52	45	49	37	39	33	33	33	38	37	33	32	32	32	34	33								
	D. rerio 1b	50	49	51	51	51	67	51	50	48	51	38	43	40	40	40	39	37	40	32	32	32	40	41	65							
	O. latipes 1	47	44	45	45	46	61	45	47	43	44	35	34	35	35	35	34	24	35	34	34	33	35	34	61	61						
	O. latipes 2	53	48	45	45	46	62	45	53	46	46	37	37	37	37	37	38	35	37	32	32	32	37	37	62	62	100					
	T. rubripes 1	53	49	48	48	48	89	48	53	45	49	39	42	36	36	36	39	36	36	35	35	35	36	35	73	64	61	63				
	T. rubripes 2	46	48	46	46	46	63	46	46	44	47	32	33	32	32	32	32	26	32	30	30	29	32	32	60	63	77	77	63			
	H. sapiens α	99	52	61	61	60	57	61	99	61	62	53	63	55	55	55	54	56	55	44	45	47	55	55	54	52	49	56	57	48		
	H. sapiens β	58	41	46	46	47	50	46	58	46	54	59	71	61	61	61	59	68	61	51	50	54	60	61	50	48	48	52	47	40	63	
	H. sapiens γ	53	48	47	47	48	51	47	53	48	46	37	44	38	38	38	38	35	38	32	33	32	38	38	50	52	50	55	55	52	54	51

The accession numbers of the sequences are reported in Table 1.

et al., 1998) are conserved in both *C. carpio* and *S. glanis* (Fig. 1A). Among teleost α-syns, two partial overlapping amino acid stretches (GAVVTGVTAVA and GVTAVAQKTVE) are the most conserved among the 11-residue repeats (Fig. 1A).

The available β-syn sequences of teleosts are composed by 115–127 amino acids. They appear well conserved, with the percentage of homology ranging from 64 (*D. rerio/S. salar*) to 100% (*A. burtoni, M. zebra, O. niloticus, P. nyererei, S. salar* 1 and 3) (Table 2). Sequence alignments showed a highly variable region in the residues 51–68 and 90–99 in *D. rerio* β-syn (Fig. 2A), whereas γ-syn sequences are 113–124 amino acids long and have a percentage of homology ranging from 60 (*D. rerio 1a/T. rubripes* 2) to 100% (*O. latipes* 1/*O. latipes* 2) (Table 2). The sequence alignment showed a wide range of variability in the C-terminal region (Fig. 2B).

Antibodies choice

On the basis of sequences analysis, we first evaluated the possible crossreactivity to carp α-syn of three antibodies directed against C-terminal epitopes of human α-syn: two noncommercial mouse monoclonal antibodies (3D5 and 2E3, Yu et al., 2007) and a polyclonal antibody (Millipore). The 3D5 antibody is directed against the epitope DMPVDPD (amino acids 115–121 in human α-syn), whereas the 2E3 recognizes the epitope QDYEP (amino acids 134–138 in human α-syn) and the polyclonal antibody is directed against the 111–131 region (Fig. 1A). In human synucleins, the epitopes recognized by the three antibodies are specific for α-syn and they are not present in β- and γ-isoform (Yu et al., 2007).

Sequence analysis showed that the epitope recognized by 3D5 antibody is perfectly conserved in carp α-syn (Fig. 1A), while it is lacking in the available teleost sequences of β- and γ-syns (Figs. 1–3). Different from 3D5, the epitope QDYEP recognized by 2E3 is not present in the partial sequence of carp α-syn nor in the other available sequences of teleost α-syn (Fig. 2A,B). The same epitope was instead identified in most available β-syn sequences from teleosts (Fig. 2). Neither β- nor γ-syn sequences are available in the carp, thus it cannot be excluded that the epitope recognized by 2E3 is present in other syn isoforms.

A

```
Cyprinus carpio      ----MKGLSKAKEGVVAAAEKTKQGVAEAAGKTKEGVLYVGSKTKEGVVHGVTTVAEKTK 56
Silurus glanis       ----MKGLSKAKEGVVAAAEKTKQGVAEAAGKTKEGVLYVGSKTKEGVVHGVTTVAEKTK 56
Homo sapiens         MDVFMKGLSKAKEGVVAAAEKTKQGVAEAAGKTKEGVLYVGSKTKEGVVHGVATVAEKTK 60
                         **************************************************:*******

Cyprinus carpio      EQVTNVGGAVVTGVTAVAQKTVEGAGSIAAATGFVKKDQLGKNEEGAPQEGILEDMPVDP 116
Silurus glanis       EQVTNVGGAVVTGVTAVAQKTVEGAGSIAAATGFVKKDQLGKNEEGAPQEGILEDMPVDP 116
Homo sapiens         EQVTNVGGAVVTGVTAVAQKTVEGAGSIAAATGFVKKDQLGKNEEGAPQEGILEDMPVDP 120
                     ************************************************************

Cyprinus carpio      DNEAYEMPS----------- 125
Silurus glanis       DNEAYEMPS----------- 125
Homo sapiens         DNEAYEMPSEEGYQDYEPEA 140
                     *********
```

B

```
Cyprinus carpio      ---------------------------------MKGLSKAKEGVVAAAEK 17
Esox lucius          MGTGYQVLQGADCIAGFEISRAKAVNWAVMDALMKGFSKAKDGVVAAAEM 50
Astatotilapia burtoni ------------------------------MDALMKGFSKAKDGVVAAAEK 21
Maylandia zebra      ------------------------------MDALMKGFSKAKDGVVAAAEK 21
Oreochromis niloticus ------------------------------MDALMKGFSKAKDGVVAAAEK 21
Oryzias latipes      ------------------------------MDVFMKGFSMAKEGVVAAAEK 21
Pundamilia nyererei  ------------------------------MDALMKGFSKAKDGVVAAAEK 21
Silurus glanis       ---------------------------------MKGLSKAKEGVVAAAEK 17
Takifugu rubripes    ------------------------------MDAFMKGFSKAKDGVVAAAEK 21
Xiphophorus maculatus ------------------------------MDALMKGFSKAKDGVVAAAEK 21
                                                     ***:* **:******* 

Cyprinus carpio      TKQGVAEAAGKTKEGVLYVGSKTKEGVVHGVTTVAEKTKEQVTNVGGAVV 67
Esox lucius          TKQGVTGAAEMTKDGVIFVGNKTKD----GVTTVAGKTVSGVSHVGGAMV 96
Astatotilapia burtoni TKQGVTGAAEMTKDGVMYVGTKTKD----GVTTVAGKTVSGVSQVGGAVV 67
Maylandia zebra      TKQGVTGAAEMTKDGVMYVGTKTKD----GVTTVAGKTVSGVSQVGGAVV 67
Oreochromis niloticus TKQGVTGAAEMTKDGVMYVGTKTKD----GVTTVAGKTVSGVSQVGEAVV 67
Oryzias latipes      TKAGMEEAAARTKEGVMYVGNKTKEGVVSSVNTVANKTVDQTNIVGDTAV 71
Pundamilia nyererei  TKQGVTGAAEMTKDGVMYVGTKTKD----GVTTVAGKTVSGVSQVGGAVV 67
Silurus glanis       TKQGVAEAAGKTKEGVLYVGSKTKEGVVHGVTTVAEKTKEQVTNVGGAVV 67
Takifugu rubripes    TKQGVTGAAEMTKDGVMFVGTKTKD----GVTVVAGKTVSGVSQVGGAMV 67
Xiphophorus maculatus TKQGVTGAAEMTKDGVMYVGTKTKD----GVSTVAEKTVSGVSHVGGAVV 67
                     ** *:  **  **:**::**.***:    .*..** ** . .. ** : *

Cyprinus carpio      TGVTAVAQKTVEGAGSIAAATGFVKKDQLGKNEEGAPQEGILEDMPVDPD 117
Esox lucius          TGVTAVAHKTVEGAGNIAAATGLVKKDPAKQEEDTLSKDSPVKESPVDTE 146
Astatotilapia burtoni TGVTAVAQKTVEGAGTIAAATGLVKKDPAKQSDDASAVQD-VAESPVDTD 116
Maylandia zebra      TGVTAVAQKTVEGAGTIAAATGLVKKDPAKQSDDASAVQD-VAESPVDTD 116
Oreochromis niloticus TGVTAVAQKTVEGAGTIAAATGLVKKDPAKQSDDASAVQD-VAESPVDTD 116
Oryzias latipes      AGAHEVSQATVEGVENVAASTGLIN-----QGEYGGMEQG--------GE 108
Pundamilia nyererei  TGVTAVAQKTVEGAGTIAAATGLVKKDPAKQSDDASAVQD-VAESPVDTD 116
Silurus glanis       TGVTAVAQKTVEGAGSIAAATGFVKKDQLGKNEEGAPQEGILEDMPVDPD 117
Takifugu rubripes    TGVTAVAQKTVESAGSIAAATGLVKKEPGKQGDDAAAPEN-MAESPDVTD 116
Xiphophorus maculatus TGVTAVAQKTVEGAGNIAAATGLVKKDPAKQGEDVSAVPD-AVESPIDTD 116
                     :*.  *:: ***.. .:**:**:::     : :      .         :

Cyprinus carpio      -NEAYEMPS---- 125
Esox lucius          GGNTTAEGHSDGY 159
Astatotilapia burtoni PADVTEEDSDE-- 127
Maylandia zebra      PADVTEEDSDE-- 127
Oreochromis niloticus PADVTEEDSDE-- 127
Oryzias latipes      GGEGY-------- 113
Pundamilia nyererei  PADVTEEDSDE-- 127
Silurus glanis       -NEAYEMPS---- 125
Takifugu rubripes    PAEATEEDADD-- 127
Xiphophorus maculatus STEPTEEDSDD-- 127
                       :
```

Figure 1. Alignment of the α-syn amino acid sequences of *Cyprinus carpio*, *Silurus glanis*, and *Homo sapiens* **(A)** and of the available teleost α-syns **(B)**. Sequences were aligned with Clustal W2. Asterisks indicate identity of amino acids; double dots indicate amino acids with the same polarity or size; dots indicate semiconserved substitutions. The epitopes recognized by the α-syn commercial polyclonal antibody (underlined), by the 3D5 monoclonal antibody (bolded), and by the 2E3 monoclonal antibody (dotted underlined) are indicated. The amino acid stretches homologous to the seven 11-residue repeats of human α-syn (Davidson et al., 1998) are alternately highlighted in gray or light gray. The 11 amino acid stretch in the hydrophobic region (GVTAVAQKTVE), characteristic of avian and mammalian α-syns, is double underlined. The accession numbers of the sequences are reported in Table 1.

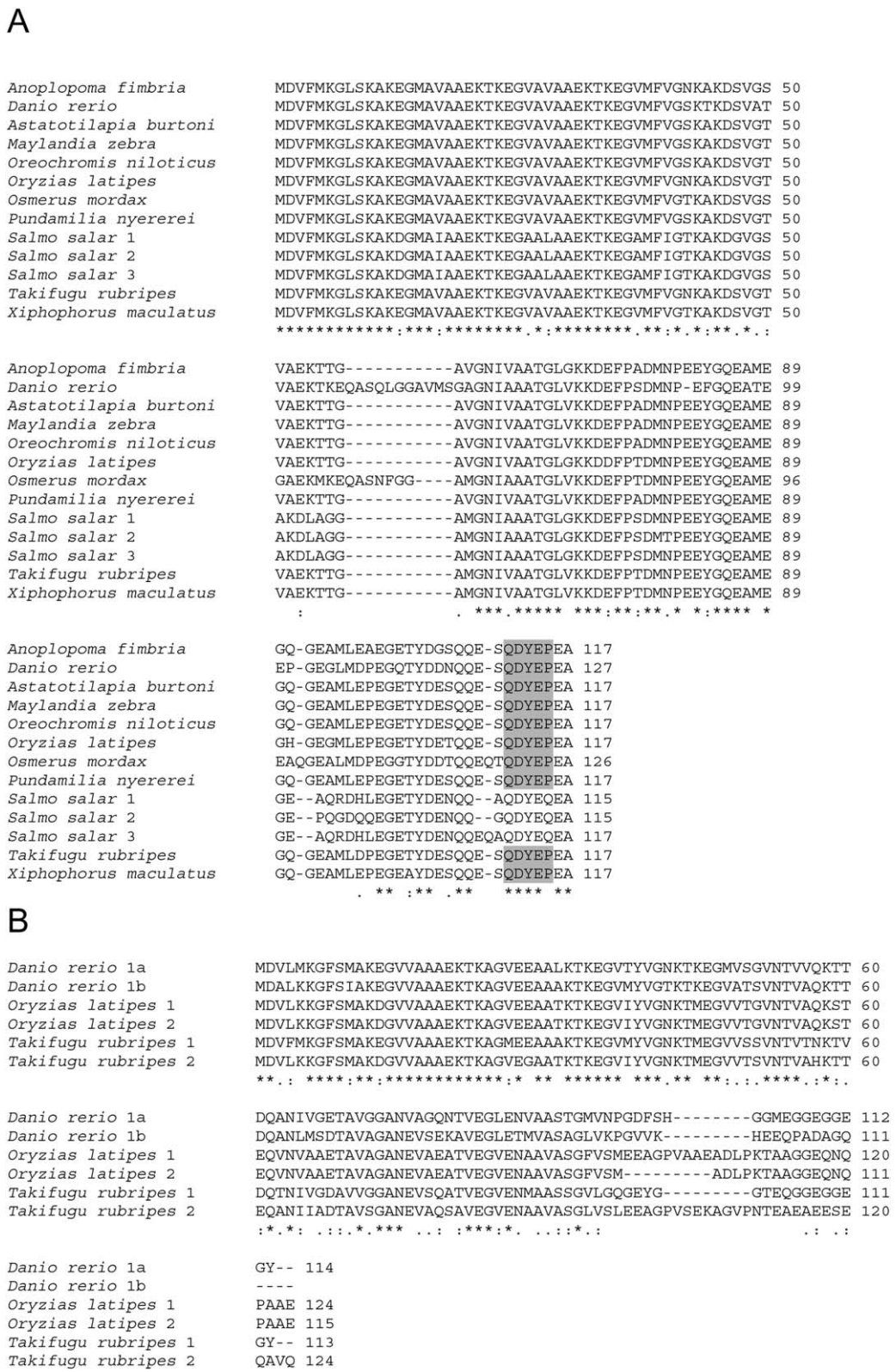

Figure 2. Alignment of the available teleost β- **(A)** and γ- **(B)** synucleins. Sequences were aligned with Clustal W2. Asterisks indicate identity of amino acids; double dots indicate amino acids with the same polarity or size; dots indicate semiconserved substitutions. The epitope recognized by the 2E3 monoclonal antibody (highlighted in gray) is indicated. The accession numbers of the sequences are reported in Table 1.

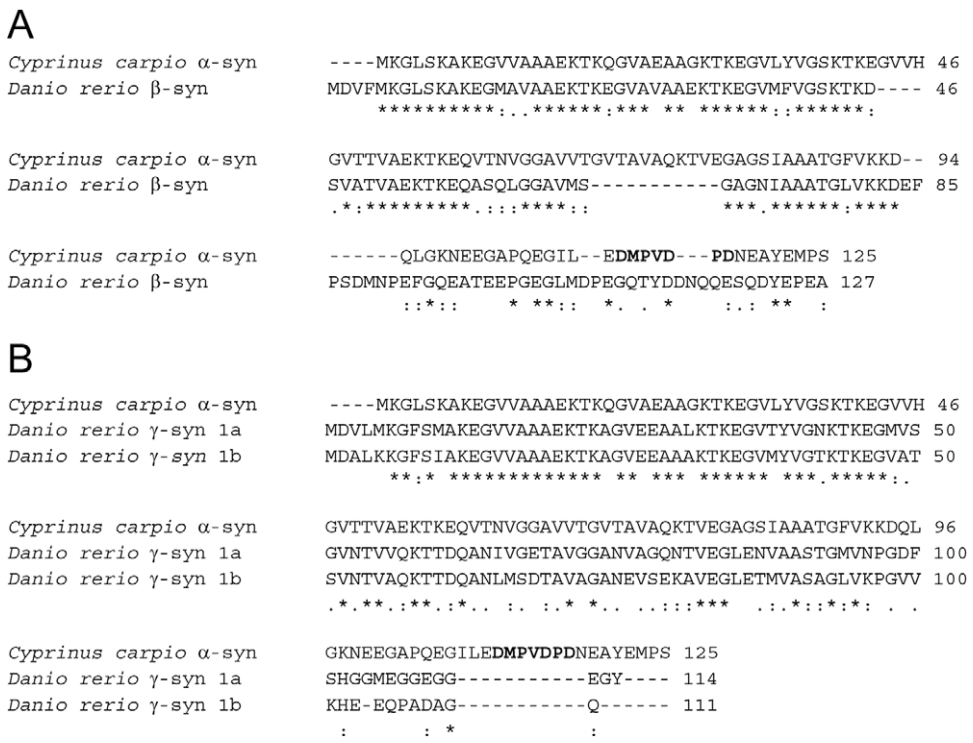

Figure 3. Alignment between the amino acid sequences of *Cyprinus carpio* α-syn and *Danio rerio* β- **(A)** and γ- **(B)** syns. Sequences were aligned with Clustal W2. Asterisks indicate identity of amino acids; double dots indicate amino acids with the same polarity or size; dots indicate semiconserved substitutions. The epitope recognized by the 3D5 monoclonal antibody is indicated bold. The accession numbers of the sequences are reported in Table 1.

The epitope recognized by the commercial polyclonal antibody is well conserved in carp α-syn with the exclusion of the last two amino acids that are not present in the partial sequence of the carp.

Validation of antibodies by western blot and immunohistochemistry

On the basis of sequence comparisons, the commercial polyclonal and the monoclonal 3D5 antibody were tested for their capacity to recognize carp α-syn by WB and IHC.

In the carp brain and spinal cord homogenates, 3D5 antibody stained a protein band at about 17 kDa corresponding with slight variations to the band labeled in the rat brain used as positive control. Additional and weaker immune-labeled bands were detected at about 12 kDa and 15 kDa (Fig. 4A). Protein bands with a molecular weight lower than 17 kDa could correspond to products of degradation, to additional isoforms, to different posttranslational modifications of α-syn like proteins, or even to unrelated proteins. Densitometric analyses of 3D5-immunolabeled bands at 17 kDa were performed on normalized actin levels (black bars in Fig. 4D). The highest α-syn-like expression was detected in the midbrain tectum, followed by the cerebellum and the diencephalon, whereas lower expression levels were found in the brainstem, the spinal cord, and the telencephalon. Given the low expression levels in these last homogenates, a longer time of film exposure was necessary to detect the 17 kDa band in the telencephalon and spinal cord (compare Fig. 4A,B).

WB analysis was repeated by using the commercial polyclonal antibody directed toward human α-syn (Millipore). This antibody detected two bands at about 15 kDa and 17 kDa in most brain samples and a weaker band at about 12 kDa in the cerebellum homogenates (Fig. 4C). Densitometric analysis of labeled bands at 17 kDa confirmed the results obtained with 3D5 antibody demonstrating that α-syn-like protein is more expressed in the midbrain tectum, the cerebellum, and the diencephalon rather than in the brainstem, the spinal cord, and the telencephalon (gray bars in Fig. 4D).

The same antibodies were tested by IHC on sections from carp and mouse spinal cord (Fig. 4E–J). In both tissues, 3D5 antibody intensely immunostained the cell bodies of motoneurons (Fig. 4E). The immunolabeling was not detected in the preadsorbed controls, in which the antibody was incubated with the recombinant human α-syn before tissue incubation (Fig. 4F).

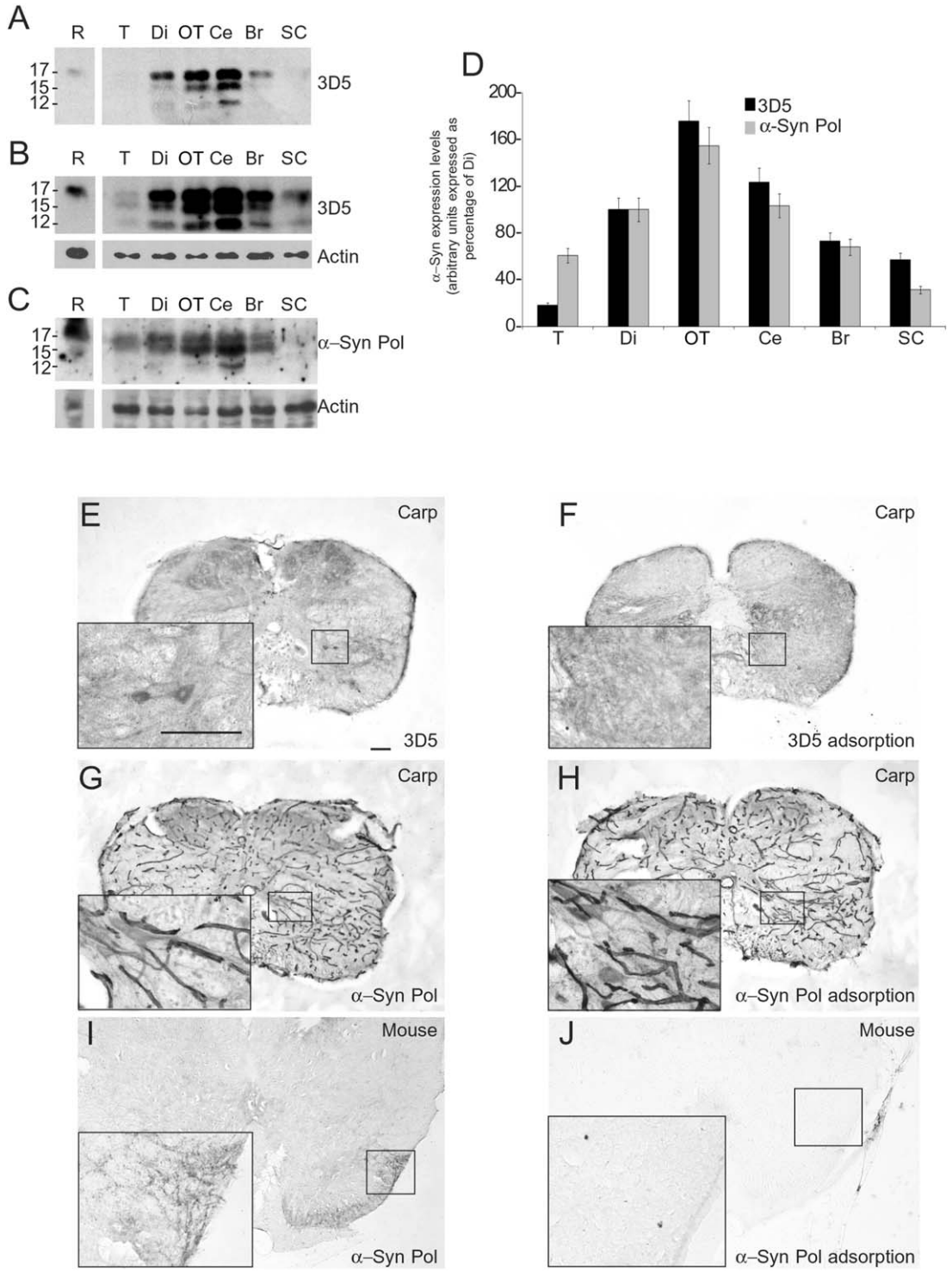

Figure 4. Regional α-syn expression in the brain and spinal cord of *Cyprinus carpio*. Expression in telencephalon (T), diencephalon (Di), midbrain tectum (OT), cerebellum (Ce), brainstem (Br), and spinal cord (SC) labeled by 3D5 antibody **(A,B)** and α-syn pol antibody **(C)**. The rat brain homogenate (R) was used as positive control and molecular weights expressed in kDa are indicated on the left. In telencephalon and diencephalon samples, a longer film exposure was necessary to detect immunolabeled bands (B). The α-syn expression was estimated by the densitometric analysis of the immunolabeled bands at 17 kDa **(D)**. Data were normalized on actin levels. Means of three values for each homogenate and standard deviation are reported. Immunohistochemistry experiments were performed in spinal cord sections from carp **(E–H)** and mouse **(I–J)** by using 3D5 **(E–F)** and α-syn pol antibody **(G–J)** to test the specificity of the antibody. Consecutive sections were incubated with the antibody (E,G,I) or with the antibody preadsorbed with human recombinant α-syn (F,H,J). Scale bars = 100 μm.

TABLE 3.

Summary of 3D5*ir* Structures in the CNS of *Cyprinus carpio* and Their Colocalization With ChAT*ir*, 5-HT*ir* and TH*ir*

			Codistribution 3D5*ir*/ChAT*ir*		Codistribution 3D5*ir*/TH*ir*		Codistribution 3D5*ir*/5HT*ir*	
3D5 positive nuclei	3D5*ir* neuronal perikarya	3D5*ir* varicose fibers	neuronal bodies	Varicose fibers	neuronal bodies	Varicose fibers	Neuronal bodies	Varicose fibers
Ventral telencephalic area, ventral nucleus (Vv)	-	++	-	x	-	-	-	-
Preoptic area (PPa, PPp, SC)	-	++	-	x	-	-	-	x
Dorsal and ventral periventricular hypothalamus (Hd, Hv)	+	++	-	x	-	-	-	-
Lateral tuberal nucleus (NLT) of the hypothalamus	-	++	-	-	-	-	-	-
Caudal hypothalamus (Hc)	+-	+	-	-	-	-	-	x
Central nucleus of the inferior lobe (NCLI)	+	+-	-	-	-	-	-	-
Ventromedial (VM) and ventrolateral (VL) thalamic nuclei	+	+	-	-	x	x	-	x
Periventricular posterior tuberculum (TPp)	+-	+	-	-	-	-	x	-
Posterior tuberal nucleus (PTN)	+-	+	-	-	-	-	x	-
Periventricular dorsal pretectum (PPd)	+-	-	-	-	x	-	-	-
Nucleus of the medial longitudinal fascicle (Nflm)	+	-	x	-	-	-	-	-
Rostral tegmental nucleus (RTN)	++	-	x	-	-	-	-	-
Superior (SR) and inferior raphe (IR)	-	++	-	-	-	x	-	x
Locus coeruleus (LC)	+	-	-	-	x	-	-	-
Cranial motor nerve nuclei III-IX	+	+	x	-	-	-	-	-
Cerebellum: ganglionic (ggl) and molecular layer (mol)	++	-	-	-	-	-	-	-
Medial octavolateral nucleus (MON)	+	+	-	-	-	-	-	-
Vagal motor lateral column (DMLX)	+	++	x	-	-	-	-	x
Superior (SRF), intermediate (IMRF) and inferior (IRF) reticular formation	+	-	x	-	-	-	-	-
Spinal cord, ventral horn (VH) and intermediate gray (IG)	++	-	x	-	-	-	-	-

+- few; + moderate; ++ abundant; x presence. -: no immunoreactive structures; +: scarce immunoreactive structures; ++: abundant immunoreactive structures.

Different from 3D5, the incubation of carp spinal cord sections with the commercial antibody produced an intense and generalized staining of blood capillaries in addition to neuronal labelings. This pattern of immunolabeling was also observed in the preadsorbed controls (Fig. 4G,H). Moreover, it was specific for the carp tissue, as the same antibody with or without the preadsorption did not produce any unspecific positive immunostaining of the capillaries in the mouse spinal cord (Fig. 4I,J), but 3D5*ir* fibers were immunolabeled (Fig. 4I).

Cellular distribution of α-syn-like proteins in the carp CNS

This analysis was performed by using 3D5 monoclonal antibody, given our preliminary evidence on its ability to stain distinct neuronal cell bodies and nerve processes in brain and spinal cord regions. The single labeling of consecutive sections with 3D5, TH, or 5HT antibodies revealed the specificity of the 3D5 immunostaining. Indeed, each antibody produced a different pattern of immunolabeling. In addition, the replacement of the primary antibody with normal serum completely abolished the immunostainings. On this basis, 3D5 immunoreactivity was considered specific for α-syn-like proteins of the carp. Colocalization of 3D5/ChAT, 3D5/TH, and 3D5/5HT was examined in selected regions by IHC/IF double immunolabeling with 3D5/ChAT, 3D5/TH, or 3D5/5HT antibodies.

Distribution of 3D5 immunoreactivity.

Neurons immunoreactive (*ir*) for 3D5 were identified in the prethalamus, tuberal region, and inferior lobes of the

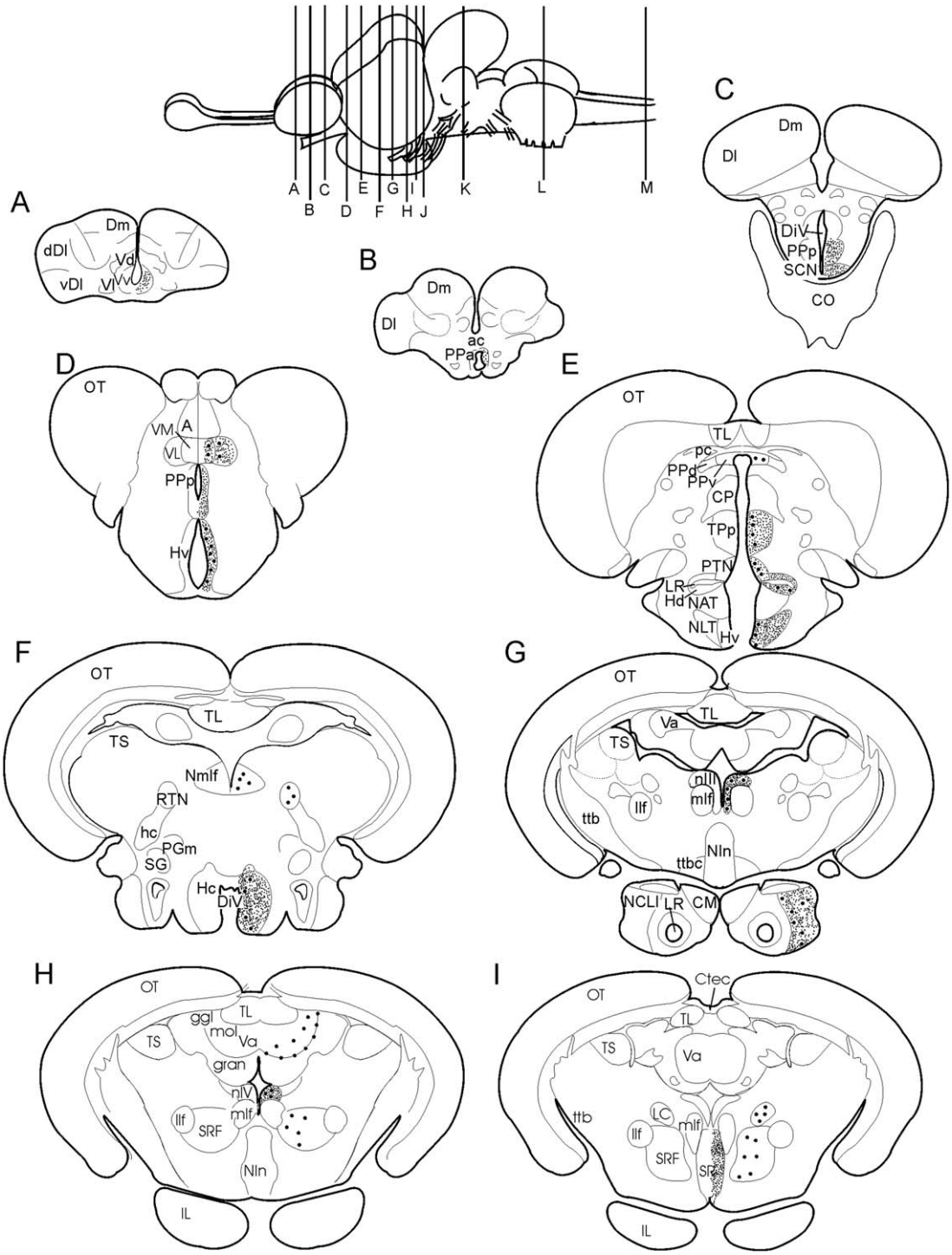

Figure 5. Schematic drawings of transverse sections through the carp brain showing the distribution of 3D5*ir* structures. Large dots indicate 3D5ir neuronal perikarya and small dots indicate 3D5ir varicose fibers.

hypothalamus, synencephalon, cerebellum, discrete brainstem nuclei, and in the spinal cord of the carp (Table 3). All the immunostained neurons showed a diffuse labeling in the perikarya and dendritic processes. Moreover, 3D5 antibody labeled thin varicose axons and the neuropil with a punctate pattern in several brain regions. Conversely, nuclear 3D5 labeling was never found in the carp neurons.

The nomenclature used for the carp brain was based on previous studies on cyprinids (Clemente et al., 2004; Mueller et al., 2004; Yamamoto and Ito, 2005a,b, 2008 in carp; Giraldez-Perez et al., 2009; Kato et al., 2012 in goldfish; Wulliman et al., 1996 in zebrafish). The distribution of 3D5 positive cells in the carp brain is depicted in the drawings of Figure 5 and summarized in Table 3.

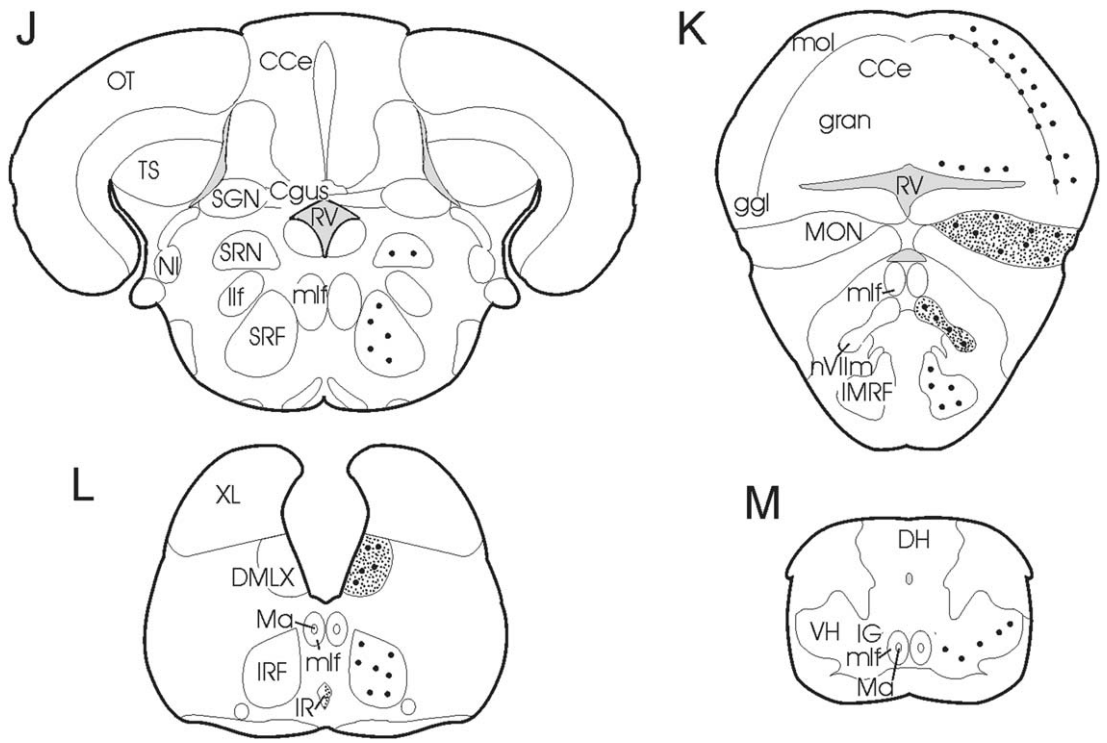

Figure 5. (continued).

Olfactory bulb

Cell bodies immunoreactive for 3D5 were not found in the olfactory bulb, which contained numerous TH*ir* neurons distributed in all cell layers and particularly in the granule layer. Abundant ChAT*ir* fibers were also present in the stratified olfactory bulb, whereas only scattered fibers were immunolabeled for 3D5 in the olfactory tract (not shown).

Telencephalon

Abundant thin axons with en passant varicosities were labeled for 3D5 in the ventral telencephalic area corresponding to the ventral nucleus (Vv) (Figs. 5A, 6A). No neuronal perikarya were stained within the Vv. However, small cells of uncertain nature were intensely stained for 3D5 in the periventricular layer (Fig. 7A). The Vv was also labeled for ChAT since a large number of ChAT*ir* varicose axons were intermingled with 3D5*ir* varicose fibers. In addition, ChAT*ir* neuronal cell bodies and dendritic processes were found on the lateral aspect of the Vv (Fig. 7A). Varicose ChAT*ir* axons were abundant in the entire subpallium. However, no immunoreactivity was found in the dorsal telencephalon for 3D5 or ChAT. The Vv of the carp was not reactive for TH, but small TH*ir* neurons were detected among the Vv, the central and the ventrolateral (Vl) nuclei of the ventral telencephalon. Double immunostaining with 3D5 and 5HT showed that 3D5*ir* thin fibers in the Vv are intermingled with serotoninergic fibers provided with large varicosities (not shown).

Preoptic area

Thin axons showing varicosities were labeled by 3D5 antibody throughout the entire preoptic region, from the anterior to the posterior nuclei (Fig. 5B–D). Labeled fibers were also detected in the horizontal region comprised between the anterior dorsal and ventral commissure (Fig. 6B). In the preoptic region neuropil, varicose 3D5*ir* axons were always codistributed with varicose ChAT*ir* axons (Fig. 7B). 3D5*ir* fibers innervated TH*ir* neurons in the preoptic nuclei and terminal 3D5*ir* varicosities were found on the cell soma and dendrites of these neurons (Fig. 7C). The preoptic region neuropil was also labeled by 5HT antibodies with a similar pattern. In fact, abundant varicose 5HT*ir* fibers were codistributed with 3D5*ir* fibers and some pictures suggested the possible colocalization of 3D5*ir* and 5HT*ir* products in the same axons (Fig. 7D). Thin varicose axons positive for 3D5 were also found in the suprachiasmatic nucleus where 3D5*ir* axons were interspersed with less numerous varicose axons positive for ChAT and varicose axons positive for 5HT (not shown).

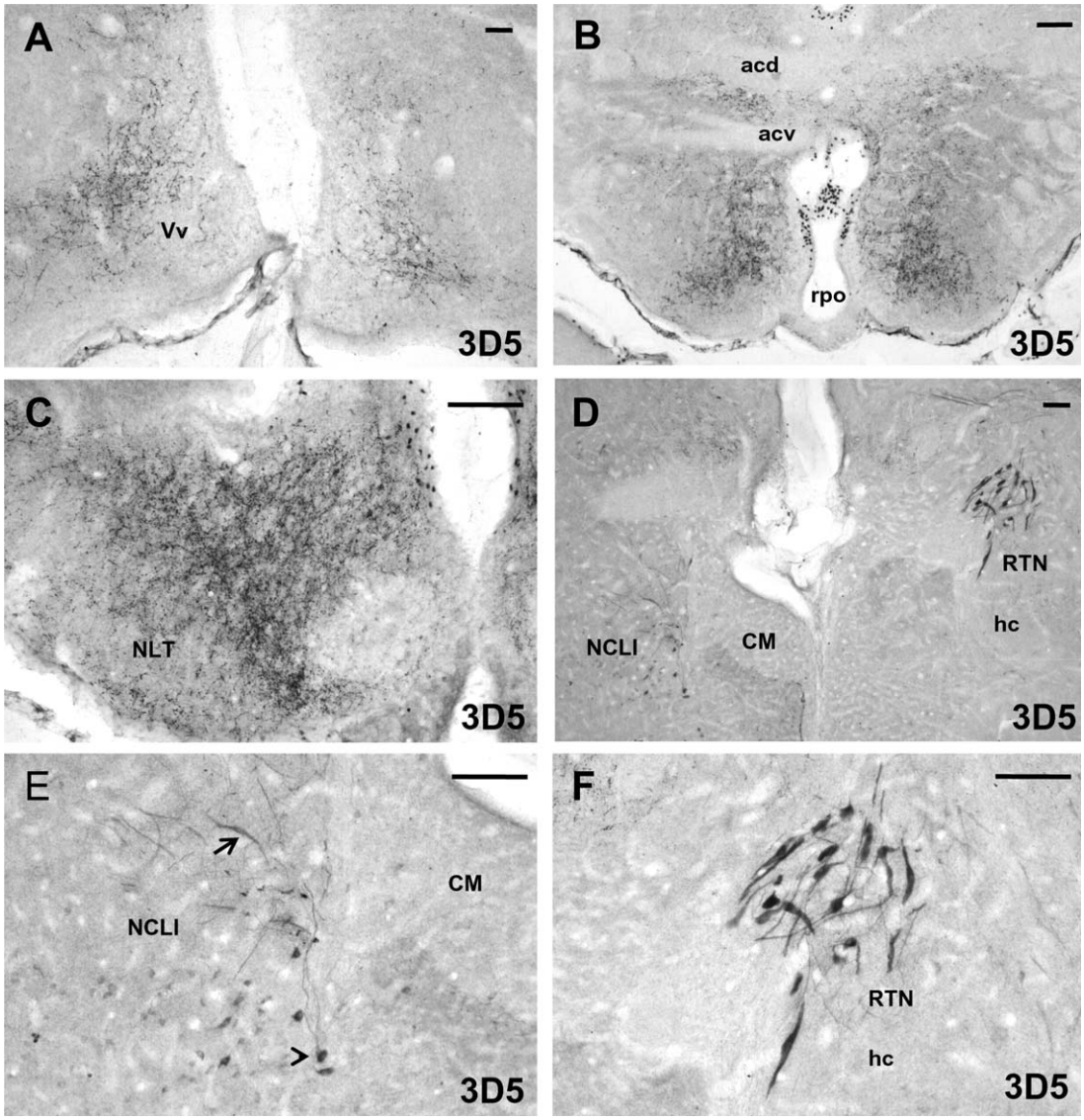

Figure 6. Immunoreactivity for 3D5 in transverse sections of the carp brain. **(A)** 3D5*ir* varicose axons are seen in the ventral nucleus of the ventral telencephalic area (Vv). Similar varicose fibers are also seen in the preoptic region **(B)** and hypothalamus **(C)**. Moreover, small cells are densely stained for 3D5 in the periventricular layer of the same regions (B). 3D5*ir* neuronal perikarya are seen in the hypothalamic NCLI **(D,E)**. Fusiform (arrow) and round cells (arrowhead) with long axons are distinguished (E). Neurons labeled for 3D5 are seen in the midbrain RTN (D,F). For other abbreviations, see list. Scale bars = 100 μm.

Hypothalamus

The immunoreactivity for 3D5 was observed in the dorsal (Hd) and ventral (Hv) periventricular hypothalamus (Fig. 5D,E). Immunoreactive products were located in numerous small perikarya and abundant varicose fibers. Some labeled cells were cerebrospinal fluid (CSF)-contacting cells while others were located at a small distance from the ventricle (Fig. 7E). In the periventricular hypothalamus, 3D5*ir* fibers were codistributed with ChAT*ir* varicose fibers. The same region was not labeled for TH or 5HT. Varicose 3D5*ir* fibers were abundant in the punctate neuropil of the lateral tuberal nucleus (NLT) (Figs. 5E, 6C). Neurons in the NLT were labeled for 5HT. 3D5*ir* varicose fibers and terminal varicosities were densely packed among these neurons (Fig. 7F). 3D5*ir* varicose fibers were abundant in the caudal hypothalamus (Hc) (Fig. 5F), which is also 5HT*ir* in the carp. In the same nucleus, scattered neuronal bodies were labeled for 3D5. Neurons were labeled by 3D5 in the central nucleus of the inferior lobe (NCLI) (Fig. 5G). Two different cell types were labeled in the inferior lobe: fusiform and round cells provided with long axons (Fig. 6D,E) that were not labeled by ChAT, TH, or 5HT antibodies.

Prethalamus

3D5 antibody labeled bipolar neurons with laterally directed axons and the surrounding punctate neuropil in

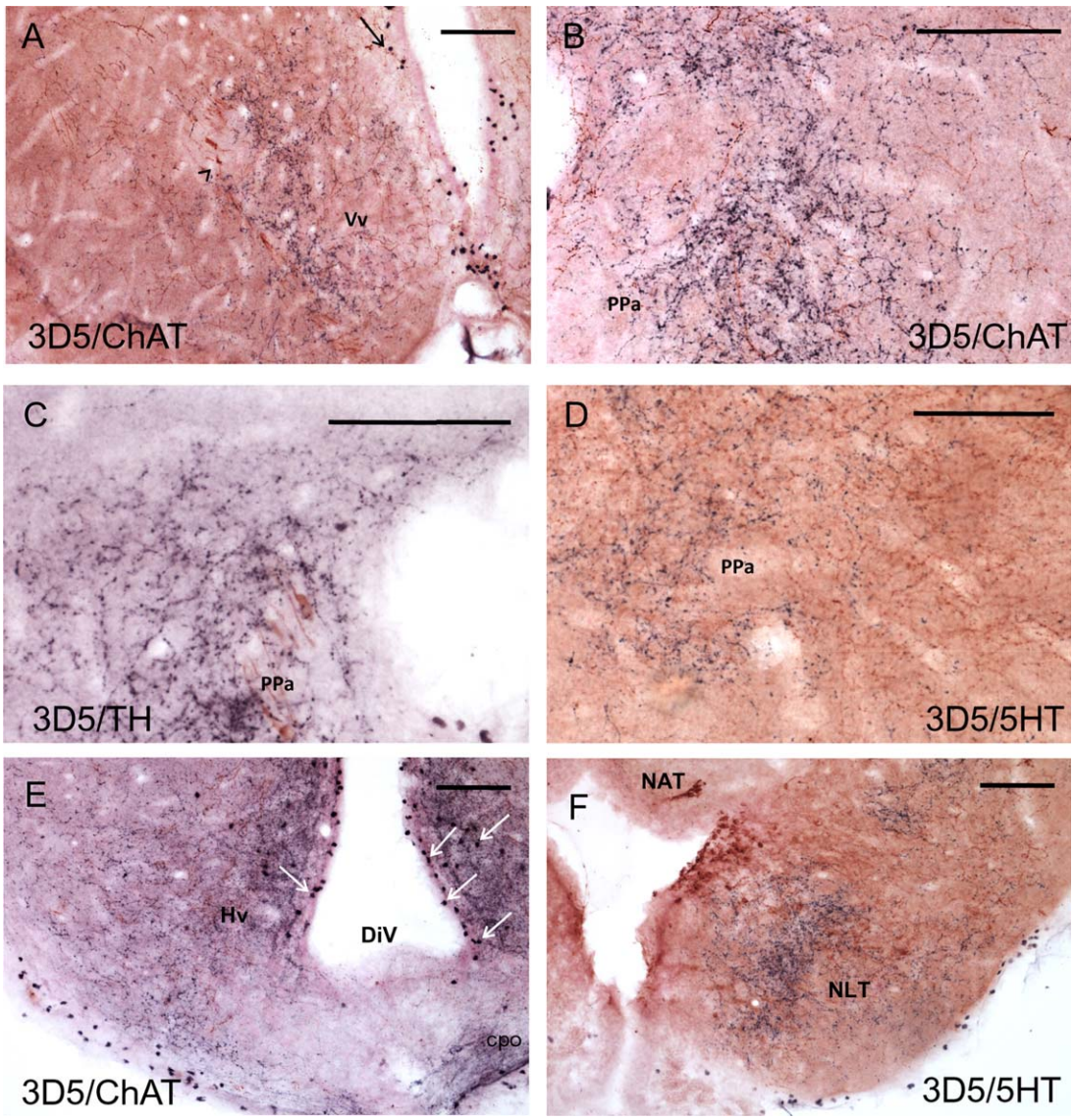

Figure 7. Double immunostaining 3D5/ChAT, 3D5/TH, and 3D5/5HT (dark-blue/brown) in transverse sections of telencephalon **(A)**, preoptic region **(B–D)** and hypothalamus **(E,F)**. A: 3D5*ir* varicose axons are codistributed with ChAT*ir* axons in the Vv. Arrow points at ChAT*ir* neuronal structures in the lateral aspect of the Vv. Arrowhead points at 3D5*ir* small cell bodies in the periventricular layer of the ventral telencephalon. B: Varicose 3D5*ir* axons are codistributed with similar ChAT*ir* axons in the PPa. C: 3D5*ir* varicosities are seen in contact with TH*ir* neurons in the PPa. D: Varicose 5HT*ir* fibers are codistributed with 3D5*ir* fibers in the parvocellular preoptic region. This distribution suggests that immunolabeled varicosities for 3D5 and 5HT are located in the same axons. E: Numerous 3D5*ir* small perikarya are seen in the periventricular Hv together with abundant varicose fibers. Labeled cells are located in contact with the ventricular surface (CSF-contacting cells) and in the subventricular layer (arrows). ChAT*ir* varicose fibers are observed among 3D5*ir* fibers. F: 3D5*ir* varicosities are densely packed in the 5HT*ir* NLT. For abbreviations, see list. Scale bars = 100 μm.

the ventrolateral (VL) and ventromedial (VM) nuclei (Figs. 5D, 8A,B). Double immunolabeling for 3D5/TH revealed that 3D5*ir* neurons are codistributed with TH*ir* neurons but evidence of 3D5/TH colocalization was not found in the same cells (Fig. 8A). The neuropil of these nuclei also contained abundant varicose 5HT*ir* axons that establish synaptic contacts on 3D5 positive neurons (not shown). The 3D5*ir* perikarya and their processes were not stained for ChAT (Fig. 8B) but they were contacted by ChAT*ir* varicosities (Fig. 8B, insert).

Thalamus

The immunoreactivity for 3D5 was limited to scattered varicose axons (not shown).

Epithalamus

The pineal organ, the habenular nuclei, and the fasciculus retroflexus were not immunoreactive for 3D5 antibody.

Posterior tuberculum

The periventricular posterior tuberculum (TPp) and the posterior tuberal nucleus (PTN) (Fig. 5E) of the carp

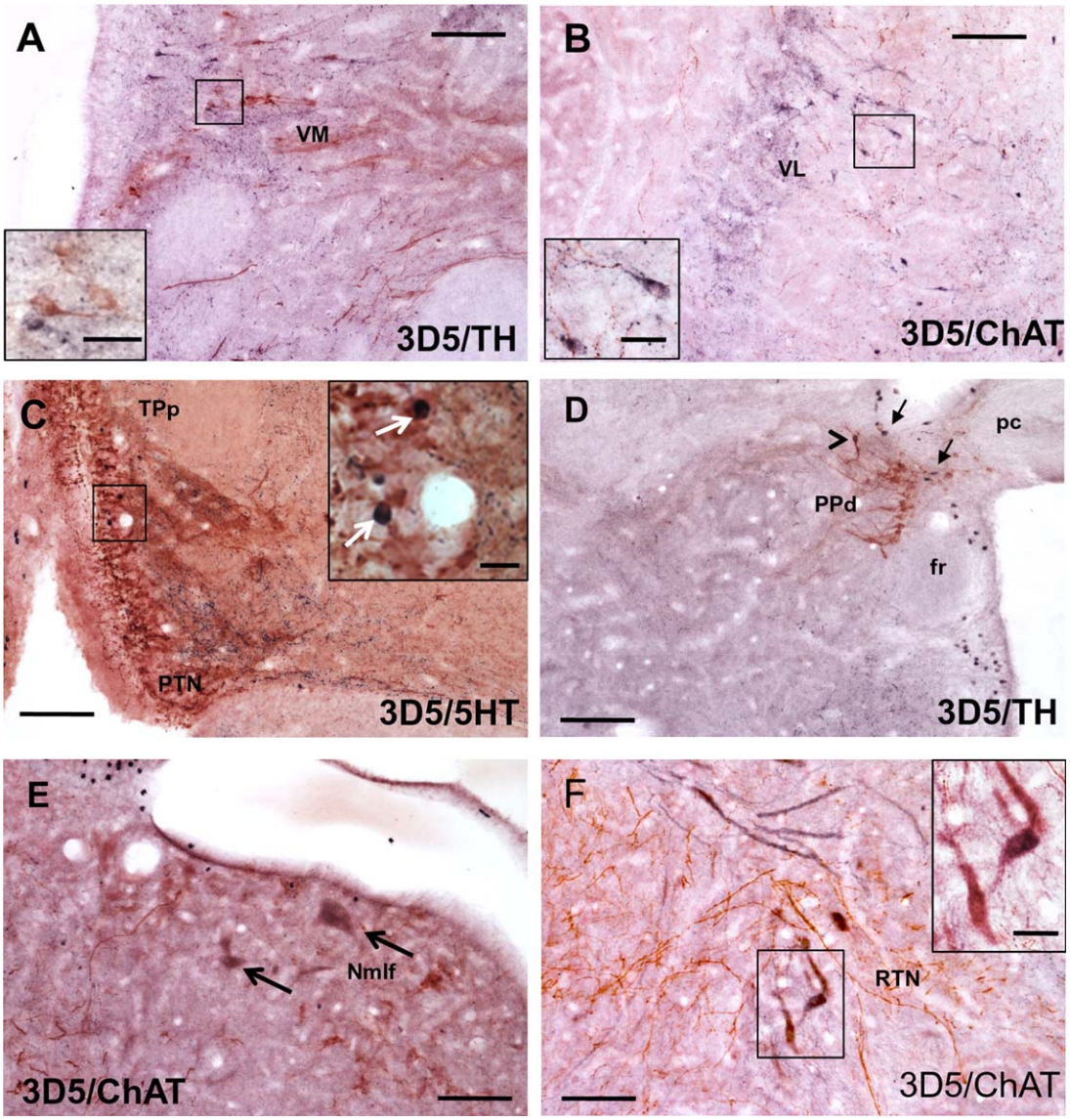

Figure 8. Double immunostaining 3D5/TH, 3D5/ChAT, and 3D5/5HT (dark-blue/brown) in ventral thalamus **(A,B)**, posterior tuberculum **(C)**, synencephalon **(D,E)** and mesencephalon **(F)**. A: 3D5*ir* neurons are seen in the VM. They are codistributed with TH*ir* neurons but no evidence of 3D5/TH colocalization was found in the same cell (detail in the insert). B: 3D5*ir* neurons in the VL are contacted by ChAT*ir* varicosities (detail in the insert). C: neurons labeled for 5HT immunoreactivity are seen in the TPp and PTN. Among them, scattered 3D5*ir* neuronal perikarya can be observed. In these neurons the colocalization of 3D5 and 5HT immunoreactive products is suggested (detail in the insert, arrows). D: Scattered neurons labeled for 3D5 are seen in the TH*ir* PPd (arrows). The 3D5/TH colocalization is suggested in some neurons (arrowhead). E: Multipolar neurons double-labeled for 3D5 and ChAT in the Nmlf (arrows). F: Bipolar neurons labeled for 3D5 are seen in the RTN. Evidence of double labeling for 3D5 and ChAT is shown in the insert. For abbreviations, see list. Scale bars = 100 μm; 25 μm in inserts.

were strongly reactive for 5HT (Fig. 8C). Among the abundant 5HT*ir* neurons, few neuronal perikarya and thin varicose axons were labeled for 3D5. The possible colocalization between 3D5 and 5HT was suggested in some neuronal bodies (Fig. 8C, insert).

Synencephalon

Neurons were labeled for 3D5 in the periventricular dorsal pretectum (PPd) (Fig. 5E), which is TH*ir* in the carp (Fig. 8D). Moreover, large and small multipolar neurons were labeled by 3D5 in the nucleus of the medial longitudinal fascicle (Nmlf) (Fig. 5F). These neurons were double-labeled by 3D5 and ChAT (Fig. 8E).

Mesencephalon

Midbrain tegmentum

Large bipolar neurons were labeled for 3D5 in a tegmental nucleus dorsomedially located to the horizontal commissure (Figs. 5F, 6D,F). This nucleus corresponds to the "rostral tegmental nucleus" (RTN) identified in

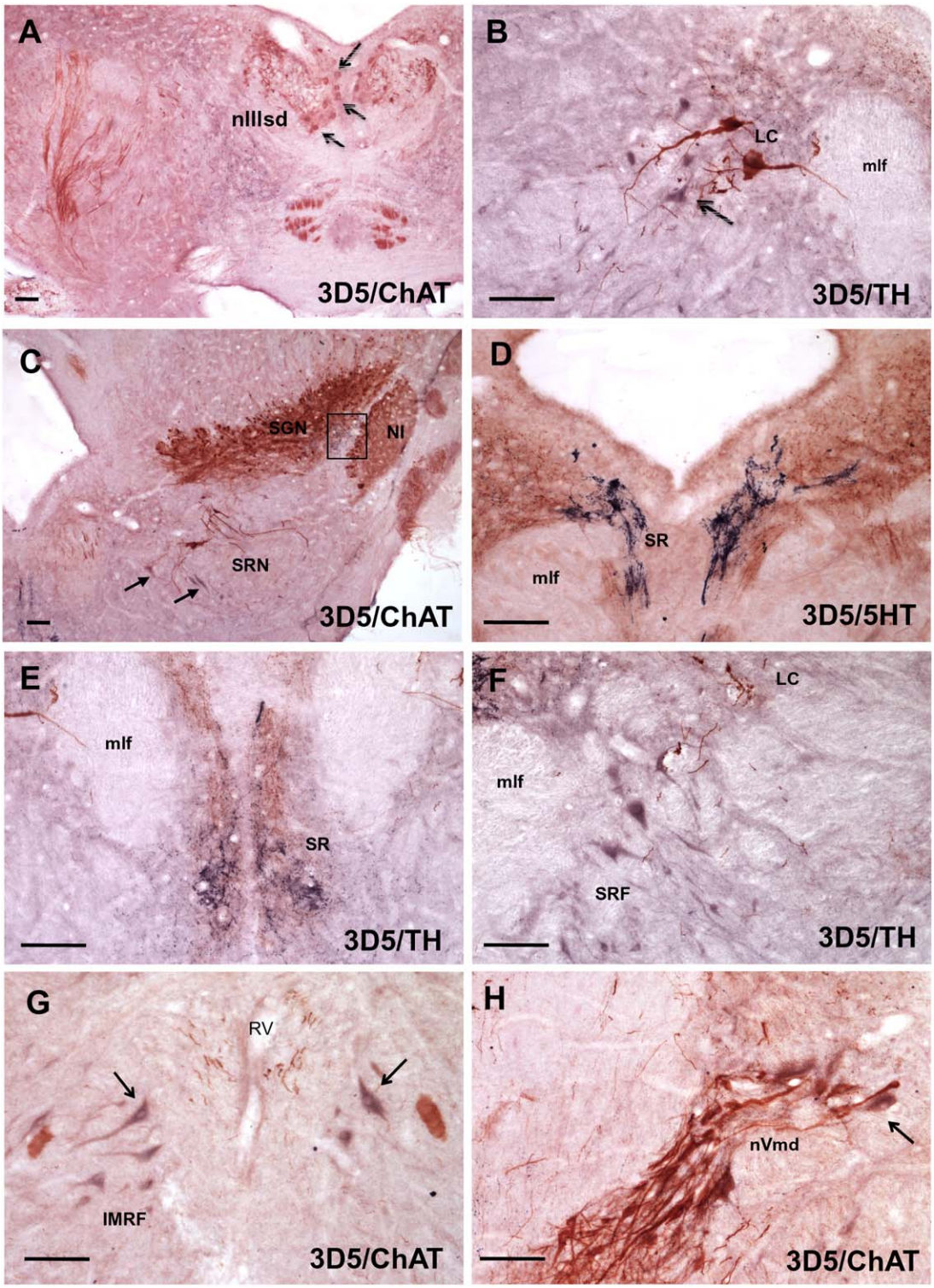

Figure 9. Double immunostaining 3D5/ChAT, 3D5/TH, and 3D5/5HT (dark-blue/brown) in transverse sections of the carp brainstem. **A:** 3D5/ChAT labeled neurons are seen within the dorsal subdivision of the oculomotor nucleus (arrows). **B:** 3D5*ir* multipolar neurons (arrow) are seen in close proximity to large TH*ir* neurons of the LC. **C:** 3D5*ir* perikarya (arrows) are seen in close proximity to the cholinergic neurons of the SRN. 3D5*ir* varicose axons are observed between ChAT*ir* SGN and NI (square box). **D:** Nerve fibers strongly immunoreactive for 3D5*ir* are intermingled with 5HT*ir* varicose fibers in the SR. **E:** 3D5*ir* axons codistributed with TH*ir* axons in the SR. **F:** Neurons reactive for 3D5 in the SRF, not labeled for TH. **G:** 3D5*ir* neurons in the IMRF, some of them double-labeled for 3D5/ChAT (arrows). **H:** 3D5 is colocalized with ChAT in some neurons in the nVmd (arrow). For abbreviations, see list. Scale bars = 100 μm.

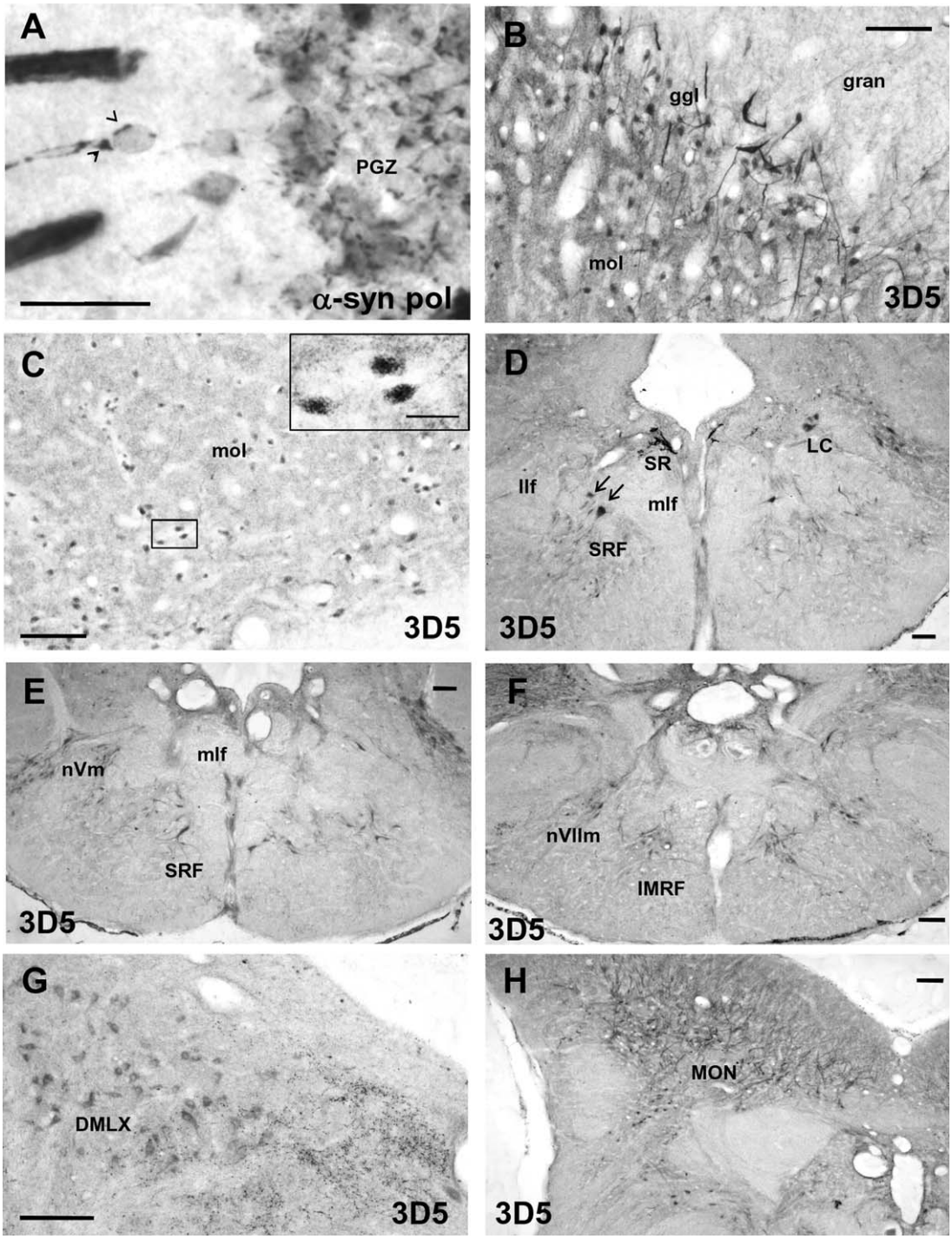

Figure 10. Transverse sections of the carp midbrain optic tectum **(A)**, cerebellum **(B,C)**, isthmus and medulla oblongata **(D–H)**, immunostained for α-syn pol (A) or 3D5 (B–H). A: α-syn pol immunoreactivity distributed in a punctate pattern on neuronal perikarya and the apical dendrite of unipolar periventricular neurons of the PGZ (arrowheads). B: Neurons immunoreactive for 3D5 in the ganglionic layer of the cerebellum. C: Small unipolar neurons labeled for 3D5 in the molecular layer of the cerebellum (detail in the insert). D: Neurons labeled for 3D5 in the SRF (arrows). E: 3D5*ir* neuronal bodies in the nVm. F: Neurons labeled for 3D5 are seen in the nVIIm and IMRF. G: Neurons reactive for 3D5 in the DMLX. H: 3D5*ir* neurons in the MON. For abbreviations, see list. Scale bars = 50 μm in A; 100 μm in B–H; 25 μm in the insert.

zebrafish (Mueller et al., 2004). The same nucleus was originally known as the "nucleus ruber tegmenti" (Goldstein, 1905) until tracer studies demonstrated that it does not correspond to the red nucleus of mammals. It was then renamed the "nucleus of the rostral mesencephalic tegmentum" (NRMT) in goldfish (Grover and Sharma, 1981) and RTN in zebrafish. A subgroup of neurons was immunostained for ChAT in the zebrafish

RTN (Mueller et al., 2004) and the same occurred in the carp. For this neurochemical similarity, the tegmental nucleus positive for 3D5 was identified as the RTN of the carp. In the double-immunostained sections, evidence of colocalization between ChAT and 3D5 immunoreactive products was obtained at the level of single neurons (Fig. 8F, insert). In the same nucleus, nerve fibers also immunoreacted for ChAT. The RTN was not reactive for TH. However, 3D5*ir* neurons were possibly contacted by thin axons and terminal varicosities positive for 5HT (not shown).

Varicose axons and terminal varicosities were strongly stained by 3D5 in the mesencephalic superior raphe region (SR) (Fig. 5I). Motor neurons of the oculomotor nucleus (nIII) and their processes were strongly immunoreactive for ChAT. Double labeling with 3D5 and ChAT antibodies revealed that some neurons in the dorsal subdivision of the nIII were stained by both ChAT and 3D5 antibodies (Fig. 9A).

Midbrain tectum.

In contrast to the intense 3D5 reactivity detected by western blot in the optic lobes homogenates, 3D5 antibody only labeled scattered varicose fibers in the optic lobes. Additional immunostainings were performed by mammalian α-syn polyclonal antibody already tested by western blot. By using this antibody, the immunostaining was detected in the periventricular gray zone (PGZ) of the midbrain tectum (Fig. 10A). α-syn pol immunoreactivity was distributed in a punctate pattern around neuronal perikarya and the apical dendrite of ChAT*ir* unipolar periventricular neurons. The granular labeling was probably due to presynaptic terminals containing α-syn-like proteins. No neuronal perikarya were immunostained for α-syn in the midbrain tectum.

Cerebellum

Neurons immunoreactive for 3D5 were found in the corpus and the valvula cerebelli. Positive cells were present in the molecular and ganglionic layers (Fig. 5H–K), whereas the granular layer was unstained. In the ganglionic layer, positive cells were numerous. Most of them showed pear-shaped perikarya and a long dendrite extending up into the molecular layer, whereas others appeared fusiform (Fig. 10B). Pear-shaped 3D5*ir* neurons might be tentatively identified as Purkinje cells. Among positive cells found in the ganglionic layer, eurydendroid neurons might be included. However, the two cell types could not be distinguished on the basis of simple morphological criteria. Small unipolar neurons positive for 3D5 were also found in the molecular layer (Fig. 10C). Since the molecular layer of teleost cerebellum contains a single type of neuronal bodies, i.e., the superficial stellate cells, 3D5*ir* neurons probably represent inhibitory stellate cells. All 3D5*ir* neurons of the carp cerebellum were unreactive for ChAT, TH, or 5HT (not shown).

Isthmus and medulla oblongata

Several cell populations were labeled for 3D5 in the hindbrain. Small multipolar neurons immunoreacted for 3D5, but not for TH, in the proximity of the large TH*ir* neurons of the locus coeruleus (LC) (Figs. 5I, 9B). In addition, 3D5*ir* cell bodies were detected in close proximity to the cholinergic neurons of the superior reticular nucleus (SRN) (Fig. 5J). In the carp, the SRN is ventromedially located to the secondary gustatory nucleus (SGN) and the nucleus isthmi (NI), which were both ChAT*ir* and received a dense net of 3D5*ir* varicose fibers (Figs. 5J, 9C).

Large and thin varicose axons were strongly stained by 3D5 throughout the superior (SR) and inferior raphe (IR) region (Fig. 5I,L). This region contained neuronal perikarya labeled for 5HT and a large number of TH*ir* and 5HT*ir* varicose axons codistributed with 3D5*ir* fibers (Fig. 9D,E). Neurons reactive for 3D5 were found in the superior (SRF), intermediate (IMRF), and inferior (IRF) rhombencephalic reticular formation (Figs. 5H–J,K,L–M, respectively, 10D–F). Positive neurons were not labeled for TH (Fig. 9F) but some of them were double stained for 3D5/ChAT (Fig. 9G).

Neurons positive for 3D5 were observed in cranial nerve motor nuclei from IV to X (Fig. 5H,K,L). Several of these nuclei also received 3D5*ir* afferent innervation made by thin varicose axons and axon terminals. In particular, both dorsal and ventral subdivisions of the trigeminal motor nucleus contained 3D5*ir* neuronal bodies (Fig. 10E). The double immunostaining with 3D5 and ChAT showed evidence that 3D5 is colocalized with ChAT in some neurons (Fig. 9H).

Similarly, both dorsal and ventral subdivisions of the facial motor nucleus (nVIIm) contained 3D5*ir* neurons (Fig. 10F) and some of them were double-labeled for 3D5/ChAT (Fig. 11A). In the facial motor nucleus 3D5*ir* neurons were innervated by 5HT*ir* axons (not shown).

Neurons reactive for 3D5 were also found in the glossopharyngeal motor nucleus and in the cholinergic lateral column of the vagal motor complex (DMLX) (Fig. 10G), where some neurons were double-labeled for 3D5/ChAT (Fig. 11B). Neuronal perikarya and fibers immunoreactive for 3D5*ir* were also seen in the medial octavolateralis nucleus (MON) (Figs. 5K, 10H).

The caudal part of the vagal lateral motor complex was richly innervated by 3D5*ir* varicose fibers belonging to the ventromedial vagal nerve root (Fig. 11C). Axonal varicosities immunolabeled for 3D5 established a large number of synaptic contacts with cholinergic neurons of this nucleus (Fig. 11D). Double immunostaining by 3D5/5HT demonstrated that the DMLX also receives serotoninergic innervation (Fig. 11E).

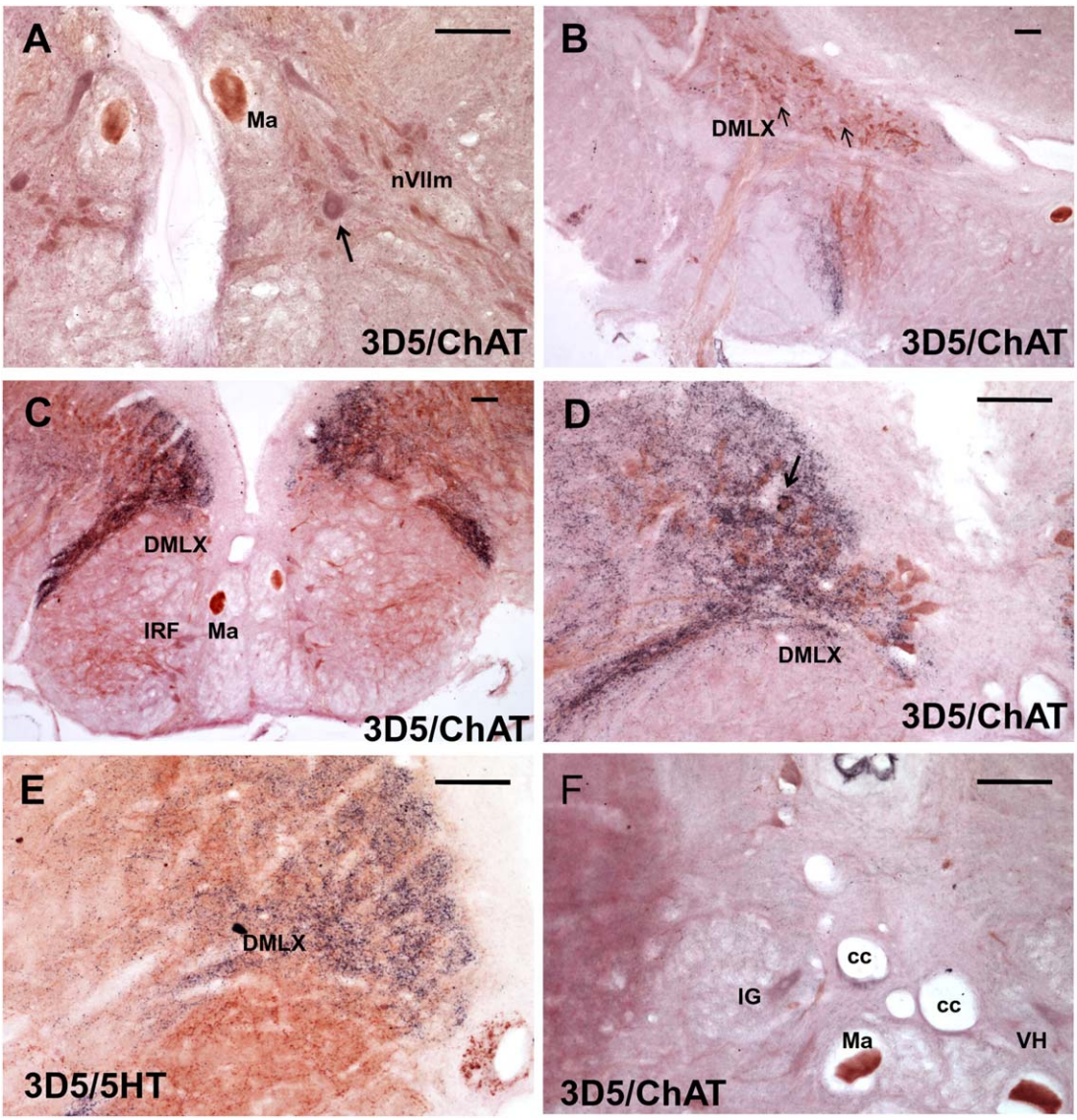

Figure 11. Transverse sections of the medulla oblongata **(A–D)** and spinal cord **(E,F)**, double immunostained for 3D5/ChAT and 3D5/5HT (dark-blue/brown). A: Neurons labeled for 3D5/ChAT are visible in the nVIIm (arrow). B: In the CMX some neurons appear double-labeled for 3D5 and ChAT (arrows). C: Cholinergic neurons of the nXm are richly innervated by 3D5ir axons belonging to the ventromedial X root. D: Axonal varicosities and synaptic contacts immunolabeled for 3D5 are seen in contact with cholinergic neurons in the DMLX (arrow). E: 3D5*ir* and 5HT*ir* varicose fibers are codistributed in the nXm. F: multipolar neurons are labeled for 3D5/ChAT in the VH and IG of the spinal cord. For abbreviations, see list. Scale bars = 100 μm.

Spinal cord

Large and small multipolar neurons were respectively stained by 3D5 in the motor column of the ventral horn (VH) and in the intermediate gray matter of the spinal cord. These cells appear to be double-labeled for 3D5 and ChAT (Figs. 5N, 11F).

Colocalization between 3D5 and ChAT immunoreactivities

Double immunofluorescence stainings with 3D5/ChAT antibodies demonstrated that 3D5 and ChAT immunoreactivities may be colocalized in the perikarya of motor neurons located in the carp brain and spinal cord. The colocalization between 3D5 and ChAT was detected within distinct neurons of the nIII (Fig. 12A–C), in the motor zone of the vagal lobe (Fig. 12D–F), and in the spinal cord motoneurons (Fig. 12G–I). Within brain cholinergic nuclei, 3D5*ir* neurons represent a minor subpopulation of ChAT*ir* neurons.

DISCUSSION

The present study demonstrates that antihuman α-syn antibodies developed against well-conserved

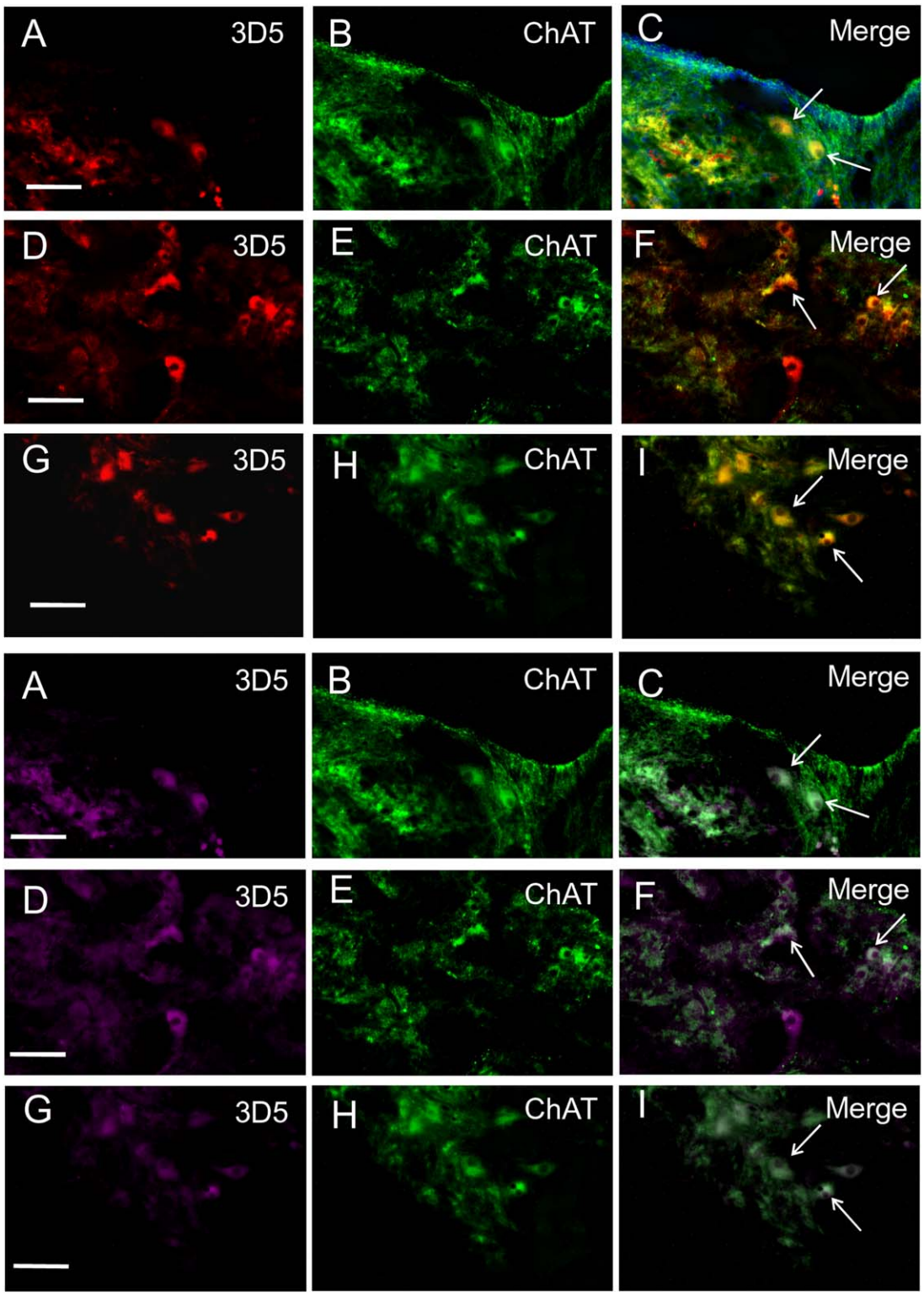

Figure 12. Double immunofluorescent stainings for 3D5/ChAT in the oculomotor nucleus **(A–C)**, the motor zone of the vagal lobe **(D–F)**, and the spinal cord **(G–I)**. The same section was immunostained with 3D5 (A,D,G) and then incubated with ChAT antibody (B,E,H). Merged images (C,F,I) clearly show the colocalization between 3D5 and ChAT in distinct neuronal bodies (arrows). Scale bars = 100 μm.

epitopes of the C-terminal tail of the human α-syn are able to recognize a protein band of about 17 kDa in the carp brain and spinal cord homogenates, which has approximately the same molecular size as that of the rat brain α-syn used as positive control. This band can be attributed to the presence of α-syn-like proteins in

the carp. The crossreactivity of the two antibodies used here for α-syn detection, a commercial polyclonal antibody (Millipore) and the noncommercial 3D5 monoclonal antibody (Yu et al., 2007), may be explained by the presence of highly conserved amino acid residues in the carboxy-terminal tail of both carp and human α-syn (Larsen et al., 2009).

Both antibodies also labeled weaker bands at 15 and 12 kDa that might correspond to degradation products, additional isoforms, or posttranslational modifications of α-syn-like protein. As the amino acid sequences of β- and γ-syns are not known in the carp, it cannot be ruled out that the 3D5 antibody in this species recognizes similar epitopes present in β- or γ-isoforms or even in unrelated proteins. Nevertheless, as shown in Figures 1–3, all the amino acid sequences of teleost β- and γ-syn available in protein databases are lacking the epitope DMPVDPD, recognized by 3D5, allowing us to suppose that the 3D5 antibody is specific for carp α-syn or α-syn-like protein.

Densitometric analysis of the immunolabeled bands at 17 kDa demonstrated that the expression levels of α-syn-like proteins differ in the main regions of the carp CNS. In particular, the highest expression was found in the midbrain tectum and the lowest in the telencephalon. A similar pattern was detected for *sncgb* (or *sncg2*, encoding γ2-syn) expression in zebrafish. Indeed, the highest levels of gene expression were found in the midbrain and hindbrain (Chen et al., 2009). With regard to α-syn, the expression levels found in the carp CNS are opposite to those found in the rat CNS, since rat α-syn is more abundant in the telencephalon and diencephalon than in the caudal brain regions (Li et al., 2002). Regional differences in α-syn expression between teleosts and mammals may be ascribed, in part at least, to the diverse evolutionary changes undergone by the forebrain and midbrain structures in the two vertebrate radiations.

In the brain and spinal cord of the carp the immunohistochemical staining by the monoclonal 3D5 antibody labeled distinct neuronal perikarya. A more significant labeling was found in the neuropil, with abundant varicose axons and terminal varicosities immunostained for α-syn throughout the CNS. The predominant α-syn localization in nerve terminals was also reported in mammals (Li et al., 2002) and the widespread presence of 3D5*ir* fibers and terminals is consistent with the major site of syn function at the presynaptic level (Maroteaux et al., 1988; Iwai et al., 1995; Li et al., 2002). The presence of a discrete number of positive neuronal perikarya in the carp suggests that α-syn accumulates in the cytoplasm of carp neurons before being transported to presynaptic terminals.

In the carp neurons, the immunoreactive material was present in perikarya, dendrites, axons, and terminal varicosities. Therefore, α-syn-like proteins appear to be ubiquitous in all cell compartments except for the nucleus. For this aspect, the cellular distribution of α-syn in the carp differs from that first identified in electromotor lobes and the electric organ of *Torpedo californica* (Maroteaux et al., 1988) since *Torpedo* syn was specifically localized to the nucleus and presynaptic terminals of cholinergic neurons. In this regard the authors suggested that nuclear α-syn might represent the unmodified protein, whereas the presynaptic protein could be the result of structural modifications occurring at the synapse or during the axonal transport. The observed differences between carp and ray may represent true differences in the α-syn cellular distribution among species or may be due to the different reactivity of the antibodies used to localize α-syn. The nuclear localization of α-syn was also controversial in normal mammalian neurons (Hegde and Jagannatha Rao, 2003) until the novel monoclonal antibody 3D5 was developed (Yu et al., 2007). This antibody was able to recognize both nuclear and presynaptic α-syn in mammalian neurons (Vivacqua et al., 2009, 2011a). In spite of its specificity for nuclear α-syn in mammals, the 3D5 antibody did not detect α-syn in the nuclear compartment of carp neurons. This negative result may reflect the true absence of nuclear α-syn or its very low expression in carp neurons. As an alternative, the epitope recognized by the 3D5 antibody might be masked by the α-syn binding to other nuclear proteins. Further studies are required to discriminate between these possible explanations. In particular, WB studies on distinct cellular fractions might help to overcome the putative effects of the epitope presentation in immunohistochemistry.

Our study demonstrated a differential distribution of 3D5*ir* structures in the main regions of the carp CNS. Double immunostainings by 3D5/TH, 3D5/5HT, and 3D5/ChAT allowed us to correlate the distribution of 3D5 immunoreactivity with those of catecholaminergic, serotoninergic, and cholinergic neurotransmitters described in cyprinids (Kah and Chambolle, 1983; Ekström, 1987; Kaslin and Panula, 2001; Clemente et al., 2004; Mueller et al., 2004; Rink and Wulliman, 2001, 2002, 2004; Giraldez-Perez et al., 2009; Yamamoto et al., 2011).

In this respect, the present results showed that the distribution of TH*ir* neurons in the carp brain is similar to that described for TH1-expressing neurons in the zebrafish brain (Yamamoto et al., 2011). In the carp brain, 3D5*ir* neuronal perikarya were codistributed with TH*ir* neurons in the prethalamus, periventricular pretectum, and locus coeruleus. Few other 3D5*ir* neurons were codistributed with 5HT*ir* neurons in the posterior

tuberculum. Moreover, 3D5*ir* varicose fibers were codistributed with similar 5HT*ir* fibers in the preoptic area, the NLT, caudal hypothalamus, prethalamus, and vagal motor nucleus. The monoaminergic region showing the highest 3D5 immunoreactivity was the raphe region, where large 3D5*ir* varicose fibers were codistributed with serotoninergic neurons and abundant 5HT*ir* or TH*ir* varicose fibers. These findings indicate that α-syn-like proteins may be expressed in few subpopulations of catecholaminergic and serotoninergic neurons in the carp brain. However, evidence of colocalization 3D5/TH or 3D5/5HT was rare at the single-cell level. Conversely, all TH*ir* cell groups expressed both *sncb* and *sncg1* (or *sncga*, encoding γ1-syn) in zebrafish (Milanese et al., 2012).

Unlike TH and 5HT, ChAT immunoreactivity was extensively codistributed and even colocalized with 3D5 immunoreactivity in the carp CNS. Neurons reactive for 3D5 were detected in cholinergic motor nuclei of the midbrain, hindbrain, and spinal cord (cranial nerve nuclei from III to X and the spinal cord motoneurons). In addition, 3D5*ir* neurons were detected in cholinergic nuclei of the synencephalon, midbrain tegmentum, and hindbrain (i.e., mlf nucleus, RTN, discrete reticular neurons). The colocalization 3D5/ChAT within the same cell was demonstrated by double immunofluorescence in the nIII and spinal cord motoneurons. In addition to neuronal perikarya, abundant varicose axons were labeled for 3D5, especially in the forebrain ventral regions (i.e., ventral telencephalic area, preoptic area, and hypothalamus) richly innervated by ChAT*ir* varicose axons. On the whole, the present results demonstrate that α-syn-like proteins are largely expressed in cholinergic systems of the carp.

The first immunohistochemical studies on mammals (Li et al., 2002; Mori et al., 2002; Lee et al., 2008) reported that α-syn is quite exclusively localized into dopaminergic or catecholaminergic neurons in general. By contrast, the recent anatomical map of the α-syn distribution in the mouse CNS made by 3D5 monoclonal antibody revealed that nuclear α-syn is almost ubiquitous. Indeed, it was found in the cholinergic, GABAergic, glutamatergic, as well as in the monoaminergic neurons (Vivacqua et al., 2011). Interestingly, the prevailing cellular localization of α-syn differs in the CNS areas so that in some regions, such as the caudate-putamen or substantia nigra, α-syn-positive neuronal nuclei were absent, while labeled fibers and synapses were abundant. The opposite was found in other regions. The authors suggested that α-syn might be implicated in multiple functions, each of them specific for a particular neuronal type (Vivacqua et al., 2011). The same explanation may be suggested for the carp CNS, i.e., the relative abundance of α-syn-like protein in fibers and synaptic terminals or into neuronal perikarya might be related to the specific functions of each neuronal subtype in the different regions.

Therefore, the prevailing α-syn expression shown by ChAT*ir* neurons in the carp does not conflict with what was previously described in mammals. The present findings sustain a functional conservation of the α-syn expression in cholinergic systems, thus suggesting that α-syn modulates similar molecular pathways in phylogenetically distant vertebrates, such as teleosts and mammals. Further studies are required to validate this suggestion, i.e., coimmunoprecipitation studies of α-syn with target proteins involved in cholinergic neurotransmission in both animal models.

The cellular distribution of α-syn in the CNS has not been investigated before in fish. Previous studies have examined the expression levels of synuclein-related transcripts in embryonic and adult tissues of zebrafish (Sun and Gitler, 2008; Chen et al., 2009). These studies reported high levels of the *sncb* (β-syn) and *sncga* (γ-syn1) mRNA in the brain and eyes. A detailed expression pattern of *sncb* and *sncg1* (=*sncga*) in the adult brain of the same species was recently reported (Milanese et al., 2012). These results demonstrated that *sncb* is expressed in the most rostral regions (olfactory bulb and dorsal telencephalon), where *sncg1* was weakly expressed. On the contrary, *sncg1* was intensely expressed in the medulla oblongata and habenula, where *sncb* expression was weak. Although the rostrocaudal distribution of α-syn expression in carp is similar to that of *sncg1* in *Danio rerio*, these results cannot be directly compared since carp β- and γ-syn sequences are still unknown. Moreover, the three genes characterized in zebrafish do not correspond to α-syn, given that the zebrafish genome lacks the α-syn sequence recognized in other teleosts. Studies on more species are necessary to understand whether the α-syn distribution observed in the carp represents the generalized condition of teleosts.

In the following sections, the α-syn distribution was compared in the carp and mammalian CNS to highlight possible similarities concerning the putative role of α-syn in vertebrates.

Forebrain

No cell bodies were labeled for 3D5 in the olfactory bulbs of the carp and only scattered 3D5*ir* fibers were found in the olfactory tracts. Olfactory bulbs of the carp were instead strongly reactive for TH, as occurs in other cyprinids. Olfactory unmyelinated axons have been traced to the ventral telencephalic area in zebrafish (Kaslin and Panula, 2001; Rink and Wulliman,

2001), which is involved in the olfactory input processing in teleosts (Meek and Nieuwenhuys, 1998). Although 3D5*ir* varicose fibers were abundant in the ventral nucleus (Vv) of the ventral telencephalon, the same fibers were not reactive for TH in the carp. This finding suggests that 3D5*ir* fibers in the ventral telencephalon originate from the more caudal region of the carp brain. In contrast, all layers of the TH*ir* olfactory bulbs exhibited positive staining for α-syn in both rat and mouse (Mori et al., 2002; Yu et al., 2007; Vivacqua et al., 2011a) and α-syn is thought to be implicated in olfactory functions in mammals.

The Vv of the carp contains ChAT*ir* neuronal bodies and varicose ChAT*ir* axons sharing similar morphology and distribution with 3D5*ir* axons. Given such similarities, it may be hypothesized that cholinergic afferents to the ventral telencephalon express α-syn. Previous studies in teleosts reported the presence of cholinergic cells limited to the ventral telencephalic area. These studies described ChAT-positive fibers with varicosities in the ventral telencephalon (Giraldez-Peres et al., 2009, in goldfish) or in the entire subpallium (Perez et al., 2000, in trout; Mueller et al., 2004; Clemente et al., 2004, in zebrafish). The ventral nuclei of the teleostean subpallium are considered homologous to part of the septum of the evaginated vertebrate brains (reviewed by Northcutt and Davis, 1983; Braford, 1995; Wullimann, 1997; Meek and Nieuwenhuys, 1998; Rink and Wulliman, 2004). Given the ubiquitous α-syn expression in the cholinergic structures of the basal forebrain in mammals (Li et al., 2002; Vivacqua et al., 2011a), the pattern of 3D5 immunoreactivity detected here suggests that the pattern of α-syn expression is conserved in the cholinergic ventral telencephalon of vertebrates.

In the carp, no labeling for 3D5 was found in the dorsal nucleus of the ventral telencephalon, which is considered part of the teleostean striatum. Conversely, intense presynaptic staining for α-syn was found in the caudate-putamen of mouse (Vivacqua et al., 2011a) accompanied to a moderate staining of neuronal nuclei in the dopaminergic substantia nigra. The comparison between carp and mouse indicates that α-syn is not expressed in teleostean structures homologous to the basal ganglia of other vertebrates.

Immunopositive fibers for 3D5 were also abundant in the preoptic region and the periventricular hypothalamus of the carp and there codistributed with ChAT*ir* varicose fibers. This confirms that cholinergic afferent projections to the forebrain may express α-syn. In the preoptic region, 3D5*ir* varicose fibers were also intermingled with 5HT*ir* fibers exhibiting the same morphology (thin beaded) and distribution. According to our findings, serotoninergic afferents to the forebrain were also described in goldfish by 5HT immunolabelings (Kah and Chambolle, 1983). These observations suggest that, in teleosts, α-syn is expressed by subpopulations of serotoninergic neurons located in the more caudal brain regions and transported along ascending axons to the preoptic region. Putative ascending 3D5*ir* projections might originate from the serotoninergic raphe region (see below) since no neurons 5HT*ir* have been detected rostrally to the hypothalamus in the carp and projections from the raphe to the forebrain have been traced in goldfish (Echteler and Saidel, 1981). A weak immunoreactivity for α-syn was detected in the preoptic and hypothalamic nuclei in mammals (Yu et al., 2007; Vivacqua et al., 2011).

Neuronal bodies expressing α-syn were identified in the periventricular hypothalamus and prethalamus (Vl and Vm nuclei) of the carp. The ventromedial nucleus was characterized in the teleost *Sebasticus marmoratus* as a multimodal relay center for the telencephalon, and afferent projections have been traced from the ventromedial thalamic nucleus to a variety of telencephalic regions, including the ventral telencephalon (Ito et al., 1986). The existence of similar projections has been postulated in zebrafish (Rink and Wulliman, 2004). On this basis, neurons labeled for 3D5 in both ventrolateral and ventromedial nuclei might represent an additional source of 3D5*ir* afferents to the ventral telencephalon of the carp. In the ventral thalamic nuclei of mammals, the α-syn expression is moderate and mainly located in the synaptic neuropil (Vivacqua et al., 2011).

Brainstem and spinal cord

Neurons positive for 3D5 were found in the midbrain tegmentum within the cholinergic RTN (previously named NRMT in goldfish). Neurons of the NRMT were found to receive inputs from the vagal lobe and to project them to the optic tectum in goldfish (Grover and Sharma, 1981). For this reason, the NRMT/RTN was considered a relay center for gustatory inputs from the vagal lobe to higher brain centers. The present evidence in the carp indicates that α-syn is expressed in gustatory circuits of the teleostean brain. Accordingly, the ventromedial vagal nerve root was extremely rich in 3D5*ir* varicose fibers in the carp (see below).

Intense α-syn-like expression was also found in the serotoninergic raphe, a region exhibiting the highest levels of 3D5 immunoreactivity in all the carp brain. Neuronal structures of the raphe also showed strong or moderate levels of α-syn expression in mammals (Vivacqua et al., 2011). In addition to raphe, small, intermediate, and large neurons were stained by 3D5 in all the subdivisions of the rombencephalic reticular formation in

the carp. In particular, neurons immunoreactive for 3D5 were detected in the isthmic cholinergic superior reticular nucleus (SRN). This nucleus has been retrogradely traced from the ventral telencephalon in zebrafish (Rink and Wulliman, 2004) and thus compared to the ascending cholinergic populations found in the brainstem of other vertebrates. In particular, the zebrafish SRN was compared to mammalian cholinergic pedunculopontine and laterodorsal tegmental nuclei, respectively projecting to the caudate-putamen and the septum (Mueller et al., 2004). The expression of α-syn in the SRN can be considered a conservative feature between teleosts and mammals, given that pontine nuclei also express α-syn in mammals (Vivacqua et al., 2011). Moreover, the SRN might be a possible source for cholinergic α-syn expressing projections to the forebrain in the carp.

A remarkable colocalization of 3D5 with ChAT immunoreactivity was found in neurons of all cranial nerve motor nuclei as well as in the somatomotor and visceromotor neurons of the spinal cord. The cholinergic nature of cranial nerve motor nuclei is a conserved feature in cyprinids (Ekström, 1987; Clemente et al., 2004; Mueller et al., 2004; Giraldez-Perez et al., 2009) as well as in other fish groups (Rodriguez-Moldes et al., 2002). The partial overlap of the two immunoreactivities in motor neurons is consistent with the first synuclein localization in the electric ray (Maroteaux et al., 1988) and the α-syn expression in mouse cholinergic neurons (Vivacqua et al., 2011a).

According to the present results, the motor zone of the vagal lobe receives abundant 3D5*ir* afferent input from the X nerve root. Since the primary afferent input to the vagal lobe is from the gustatory portion of the vagal nerve (Farrell et al., 2002), this suggests that α-syn is involved in synaptic transmission of special viscerosensory gustatory inputs in teleosts as well as in mammals, where abundant 3D5*ir* cell nuclei in the nucleus of the solitary tract were shown (Vivacqua et al., 2011a).

Midbrain tectum

According to the WB results, large amounts of α-syn-like proteins are expressed in the midbrain tectum. However, the 3D5 antibody was not able to reveal the cellular localization of α-syn by immunohistochemistry. This negative result could be ascribed to the binding/interaction of α-syn with specific proteins or to the polymerization of α-syn molecules. Both of these conditions could cause the masking of the epitope recognized by 3D5 antibody. Such an explanation is confirmed by the immunostainings with the α-syn polyclonal antibody that was able to detect a strong α-syn expression at the presynaptic level in the periventricular layer. Based on this evidence, α-syn appears to be predominantly expressed at the synaptic level in the midbrain tectum. A moderate labeling for nuclear α-syn was reported in several layers of the superior colliculus in mammals (Vivacqua et al., 2011).

Cerebellum

Neuronal perikarya were labeled for 3D5 in the ganglionic and molecular layers of the carp cerebellum. On the basis of morphological criteria, 3D5-positive cells could be identified as Purkinje neurons and stellate cells. No neurons were labeled for ChAT in the carp cerebellum. Similarly, no ChAT*ir* neurons are present in the zebrafish cerebellum (Clemente et al., 2004), whereas ChAT-labeled cells were detected in the ganglionic layer of goldfish cerebellum (Giraldez-Perez et al., 2009). Given the relative high number of 3D5-positive neurons in the carp cerebellum, the present data suggest that α-syn may be involved in specific functions within cerebellar circuits of teleosts. Such functions might be conserved in vertebrates, since a strong staining for α-syn was also found in the Purkinje and molecular layers of human (Mori et al., 2002) and mouse cerebellum (Vivacqua et al., 2011a). Interestingly, *g1-syn* is also expressed in the Purkinje cells of zebrafish cerebellum, whereas *sncb* is expressed in the granule cells (Milanese et al., 2012).

CONCLUSION

The present results demonstrate that significant amounts of α-syn-like proteins are expressed in the neuronal perikarya, axoplasm, and presynaptic terminals of neurons localized in several brain regions and the spinal cord of the common carp. α-syn-like proteins appear to be preferentially expressed by cholinergic neurons and thus participate in cholinergic neurotransmission in teleosts.

The immunohistochemical detection of α-syn-like proteins at presynaptic terminals suggests that presynaptic functions of α-syn are evolutionarily conserved. α-syn is particularly involved in the synaptic transmission at the presynaptic level (Cheng et al., 2011). In this regard, it is noteworthy that the few sequenced α-syns from teleosts share the same hydrophobic N-terminal with mammalian α-syn. In particular, all the α-syn sequenced from *C. carpio*, *H. burtoni*, *M. zebra*, *O. niloticus*, *P. nyererei*, *S. glanis*, *T. rubripes*, and *X. maculatus* possess the typical 11 amino acid stretch in the hydrophobic region (GVTAVAQKTVE), which is 100% conserved in comparison to human α-syn (Yoshida et al., 2006). This suggests that the lipid binding is a conserved biochemical property of all known α-syns. Lipid binding is crucial for α-syn interaction with synaptic vesicles and its

consequent regulation of synaptic transmission (Volles and Lansbury, 2007; Yang et al., 2010).

In conclusion, the present results propose a new vertebrate model for studying the biological function of α-syn. The specific colocalization between carp α-syn and ChAT may open future perspectives to the development of a new model of α-syn-mediated neurodegeneration based on a selective degeneration of cholinergic neurons. Several synucleinopathies indeed are characterized by the degeneration of cholinergic neurons, which are also the main target in the Alzheimer's disease.

ACKNOWLEDGMENT

We thank Prof. Ebe Parisi Salvi for suggestions and advice in the achievement of this work.

CONFLICT OF INTEREST

The authors declare no conflict of interest.

ROLE OF AUTHORS

All authors had full access to all the data in the study and take responsibility for the integrity of the data and accuracy of the data analysis. Study concept and design: L. D'Este, G. Vivacqua; Acquisition data: A. Casini, M. Toni, R. Vaccaro; Analysis and interpretation of data: C. Cioni, M. Toni, R. Vaccaro; Drafting of the article: C. Cioni, M. Toni, R. Vaccaro, G. Vivacqua; Critical revision of the article for important intellectual content: S. Yu; Statistical analysis: M. Toni; Obtained funding: M. Toni; Administrative, technical and material support: A. Casini, M. Toni; Study supervision: C. Cioni.

LITERATURE CITED

Adjou KT, Allix S, Ouidja MO, Backer S, Couquet C, Cornuejols MJ, Desyls JP, Brugère H, Brugère-Picoux J, El-Hachimi KH. 2007. Alpha-synuclein accumulates in the brain of scrapie-affected sheep and goats. J Comp Pathol 137:78–81.

Al-Chalabi A, Durr A, Wood NW, Parkinson MH, Camuzat A, Hulot JS, Morrison KE, Renton A, Sussmuth SD, Landwehrmeyer BG, Ludolph A, Agid Y, Brice A, Leigh PN, Bensimon G. 2009. Genetic variants of the α-synuclein gene SNCA are associated with multiple system atrophy. PLoS One 4:e7114.

Alim MA, Ma QL, Takeda K, Aizawa T, Matsubara M, Nakamura M, Asada A, Saito T, Kaji H, Yoshii M, Hisanaga S, Uéda K. 2004. Demonstration of a role for alpha-synuclein as functional microtubule-associated protein. J Alzheimers Dis 6:435–442.

Boudreau H, Krol KM, Eibl JK, Williams LD, Rossiter JP, Palace VP, Ross GM. 2009. The association of metal ion exposure with α-synuclein-like immunoreactivity in the central nervous system of fish, *Catostomus commersoni*. Aquat Toxicol 92:258–263.

Braford MR. 1995. Comparative aspects of forebrain organization in the ray-finned fishes: touchstone or not? Brain Behav Evol 46:259–274.

Bricaud O, Chaar V, Dambly-Chaudière C, Ghysen A. 2001. Early efferent innervations of the zebrafish lateral line. J Comp Neurol 434:253–261.

Burré J, Sharma M, Tsetsenis T, Buchman V, Etherton MR, Sudhof TC. 2010. Alpha-synuclein promotes SNARE-complex assembly in vivo and in vitro. Science 329: 1663–1667.

Carlson SS, Kelly RB. 1980. An antiserum specific for cholinergic synaptic vesicles from electric organ. J Cell Biol 87:98–103.

Chandra S, Fornai F, Kwon HB, Yazdani U, Atasoi D, Liu X, Hammer RE, Battaglia G, German DC, Castillo PE, Sudhof TC. 2004. Double knockout mice for α- and β-synucleins. Effect on synaptic functions. Proc Natl Acad Sci U S A 101:14966–14971.

Chen YC, Cheng CH, Chen GD, Hung CC, Yang CH, Hwang SP, Kawakami K, Wu BK, Huang CJ. 2009. Recapitulation of zebrafish sncga expression pattern and labeling the habenular complex in transgenic zebrafish using green fluorescent protein reporter gene. Dev Dyn 238:746–754.

Cheng F, Vivacqua G, Yu S. 2011. The role of α-synuclein in neurotransmission and synaptic plasticity. J Chem Neuroanat 42:242–248.

Clemente D, Porteros A, Weruaga E, Alonso JR, Arezana JF, Aijon J, Arevalo R. 2004. Cholinergic elements in zebrafish central nervous system: histochemical and immunohistochemical analysis. J Comp Neurol 474:75–107.

Davidson WS, Jonas A, Clayton DF, George JM. 1998. Stabilization of alpha-synuclein secondary structure upon binding to synthetic membranes. J Biol Chem 273:9443–9449.

Dezfuli BS, Giari L, Simoni E, Shinn AP, Manera M, Bosi G. 2005. Histopathology, ultrastructure and immunohistochemistry of *Coregonus lavaretus* hearts naturally infected with *Ichthyocotylurus erraticus* (Trematoda). Dis Aquat Organ 66:245–254.

Dezfuli BS, Giovinazzo G, Lui A, Giari L. 2008. Inflammatory response to *Dentitruncus truttae* (*Acanthocephala*) in the intestine of brown trout. Fish Shellfish Immunol 24:726–733.

Echteler SM, Saidel WM. 1981. Forebrain connections in the goldfish support telencephalic homologies with land vertebrates. Science 212:683–685.

Ekström P. 1987. Distribution of choline acetyltransferase-immunoreactive neurons in the brain of a cyprinid teleost (*Phoxinus phoxinus L.*). J Comp Neurol 256:494–515.

Ekström P, Honkanen T, Steinbusch HW. 1990. Distribution of dopamine-immunoreactive neuronal perikarya and fibres in the brain of a teleost, *Gasterosteus aculeatus L*. comparison with tyrosine hydroxylase- and dopamine-beta-hydroxylase-immunoreactive neurons. J Chem Neuroanat 3:233–260.

Farrel WJ, Bottger B, Ahmadi F, Finger TE. 2002. Distribution of cholecystokinin, calcitonin gene-related peptide, neuropeptide Y, and galanin in the primary gustatory nuclei of the goldfish. J Comp Neurol 450:103–114.

Flinn L, Bretaud S, Lo C, Ingham PW, Bandmann O. 2008. Zebrafish as a new animal model for movement disorders. J Neurochem 106:1991–1997.

Funakoshi K, Nakano M, Atobe Y, Kadota T, Goris RC, Kishida R. 2002. Catecholaminergic innervation of the sympathetic preganglionic cell column of the filefish *Stephanolepis cirrhifer*. J Comp Neurol 442:204–216.

Giraldez-Perez RM, Gaytan SP, Torres B, Pasaro R. 2009. Colocalization of nitric oxide synthase and choline acetyltransferase in the brain of the goldfish (*Carassius auratus*). J Chem Neuroanat 37:1–17.

Goers J, Manning-Bog AB, McCormack AL, Millett IS, Doniach S, Di Monte DA, Uversky VN, Fink AL. 2003. Nuclear localization of alpha-synuclein and its interaction with histones. Biochemistry 42:8465–8471.

Goldstein K. 1905. Untersuchung ûber das Vorderhirn und Zwischenhirn einiger Knochenfische nebsten einiger Beiträgen ûber Mittelhirn und Kleinhirn derselben. Arch Mikros Anat 66:135–219.

Greten-Harrison B, Polydoro M, Morimoto-Tomita M, Diao L, Williams AM, Nie EH, Makani S, Tian N, Castillo PE, Buchman VL, Chandra SS. 2010. $\alpha\beta\gamma$-Synuclein triple knockout mice reveal age-dependent neuronal disfunction. Proc Natl Acad Sci U S A 107:19573–19578.

Grover BG, Sharma SC. 1981. Organization of extrinsic tectal connections in goldfish (*Carassius auratus*). J Comp Neurol 196:471–488.

Hamilton BA. 2004. Alpha-synuclein A53T substitution associated with Parkinson disease also marks the divergence of Old World and New World primates. Genomics 83: 739–742.

Hedge ML, Jagannatha Rao KS. 2003. Challenges and complexities of α-synuclein toxicity: new postulates in unfolding the mistery associated with Parkinson's disease. Arch Biochem Biophys 418:169–178.

Hornby PJ, Piekut DT. 1990. Distribution of catecholamine-synthesizing enzymes in goldfish brains: presumptive dopamine and norepinephrine neuronal organization. Brain Behav Evol 35:49–64.

Ito H, Murakami T, Fukuoka T, Kishida R. 1986. Thalamic fiber connections in a teleost (*Sebastiscus marmoratus*): visual somatosensory octavolateral, and cerebellar relay region to the telencephalon. J Comp Neurol 250:215–227.

Iwai A, Masliah E, Yoshimoto M, Ge N, Flanagan L, de Silva HA, Kittel A, Saitoh T. 1995. The precursor protein of non-A beta component of Alzheimer's disease amyloid is a presynaptic protein of the central nervous system. Neuron 14:467–475.

Jellinger KA. 2011. Interaction between pathogenic proteins in neurodegenerative disorders. J Cell Mol Med 16:1166–1183.

Jenco JM, Rawlingson A, Daniels B, Morris AJ. 1998. Regulation of phospholipase D2: selective inhibition of mammalian phospholipase D isoenzyme by alpha- and beta-synucleins. Biochemistry 37:4901–4909.

Kah O, Chambolle P. 1983. Serotonin in the brain of the goldfish, *Carassius auratus*. An immunocytochemical study. Cell Tissue Res 234:319–333.

Kanaan NM, Manfredsson FP. 2012. Loss of functional alpha-synuclein: a toxic event in Parkinson's disease? J Parkinsons Dis 2:249–267.

Kaslin J, Panula P. 2001. Comparative anatomy of the histaminergic and other aminergic systems in zebrafish (Danio rerio). J Comp Neurol 440:342–377.

Kato T, Yamada Y, Yamamoto N. 2012. Ascending gustatory pathways to the telencephalon in goldfish. J Comp Neurol 520:2475–2499.

Kumar S, Singh U, Saha S, Singru PS. 2014. Tyrosine hydroxylase in the olfactory system, forebrain and pituitary of the Indian major carp, *Cirrhinus cirrhosus*: organisation and interaction with neuropeptide Y in the preoptic area. J Neuroendocrinol 26:400–411.

Laemmli UK. 1970. Cleavage of structural proteins during the assembly of the head of bacteriophage T4. Nature 227: 680–685.

Larsen K, Hedegaard C, Bertelsen MF, Bendixen C. 2009. Threonine 53 in α-synuclein is conserved in long-living non-primate animals. Biochem Biophys Res Commun 387:602–605.

Lee SJ, Jeon H, Kandror KV. 2008. Alpha-synuclein is localized in a subpopulation of rat brain synaptic vesicles. Acta Neurobiol Exp 68:509–515.

Li JY, Henning Jensen P, Dahlstrom A. 2002. Differential localization of alpha-, beta-, and gamma-synucleins in the rat CNS. Neuroscience 113:463–478.

Lowry OH, Rosebrough NJ, Farr AL, Randall RJ. 1951. Protein measurement with the Folin phenol reagent. J Biol Chem 193:265–275.

Maroteaux L, Campanelli JT, Scheller RH. 1988. Synuclein: a neuron-specific protein localized to the nucleus and presynaptic nerve terminal. J Neurosci 8:2804–2815.

Martin LJ, Pan Y, Price AC, Sterling W, Copeland NG, Jenkins NA, Price DL, Lee MK. 2006. Parkinson's disease α-synuclein transgenic mice develop neuronal mitochondrial degeneration and cell death. J Neurosci 26:41–50.

Martinez-Navarrete GC, Martin-Nieto J, Esteve-Rudd J, Angulo A, Cuenca N. 2007. α-Synuclein gene expression profile in the retina of vertebrates. Mol Vis 13:949–961.

Matsui H, Taniguchi Y, Inoue H, Takeda S, Takahashi R. 2009. A chemical neurotoxin, MPTP induces Parkinson's disease like phenotype movement disorders and persistent loss of dopamine neurons in medaka fish. Neurosci Res 65:263–271.

Matsui H, Inoue H, Kobayashi Y, Sakaki Y, Toyoda A, Uemura K, Kobayashi D, Takeda S, Takahashi R. 2010. Loss of PINKI in medaka fish (*Oryzias latipes*) causes late-onset decrease in spontaneous movement. Neurosci Res 66: 151–161.

Meek J, Nieuwenhuys R. 1998. Holosteans and teleosts. In: Nieuwenhuys R, ten Donkelaar HJ, Nicholson C, editors. The central nervous system of vertebrates, vol. 2. Berlin: Springer. p 759–937.

Meek J, Joosten HW, Hafmans TG. 1993. Distribution of noradrenaline-immunoreactivity in the brain of the mormyrid teleost *Gnathonemus petersii*. J Comp Neurol 328: 145–160.

Milanese C, Sager JJ, Bai Q, Farrel TC, Cannon JR, Greenamyre JT, Burton EA. 2012. Hypokinesia and reduced dopamine levels in zebrafish lacking β- and γ-synucleins. J Biol Chem 5:2971–2983.

Mori F, Tanji K, Yoshimoto M, Takahashi H, Wakabayashi K. 2002. Immunohistochemical comparison of α- and β-synuclein in adult rat central nervous system. Brain Res 941:118–126.

Morita Y, Finger TE. 1987. Area postrema of the goldfish, *Carassius auratus*: ultrastructure, fiber connections, and immunocytochemistry. J Comp Neurol 256:104–116.

Mueller T, Vernier P, Wullimann MF. 2004. The adult central nervous cholinergic system of a neurogenetic model animal, the zebrafish *Danio rerio*. Brain Res 1011:156–169.

Mukuda T, Matsunaga Y, Kawamoto K, Yamaguchi K, Ando M. 2005. Blood-contacting neurons in the brain of the Japanese eel *Anguilla japonica*. J Exp Zool A Comp Exp Biol 303:366–376.

Neystat M, Rzhetskaya M, Kholodilov N, Burke RE. 2002. Analysis of synphillin-1 and synuclein interactions by yeast two-hybrid beta-galactosidase liquid assay. Neurosci Lett 325:119–123.

Northcutt RG. 2006. Connections of the lateral and medial divisions of the goldfish telencephalic pallium. J Comp Neurol 494:903–943.

Northcutt RG, Davis RE. 1983. Telencephalic organization in ray-finned fishes. In: Davis RE, Northcutt RG, editors. Fish neurobiology, vol. 2. Higher brain areas and

functions. Ann Arbor, MI: University of Michigan Press. p 203–236.

Nunes-Tavares N, Cunha-E-Silva NL, Hassón-Voloch A. 2000. Choline acetyltransferase detection in normal and denervated electrocyte from Electrophorus electricus (L.) using a confocal scanning optical microscopy analysis. An Acad Bras Cienc 72:331–340.

O'Connell LA, Fontenot MR, Hofmann HA. 2013. Neurochemical profiling of dopaminergic neurons in the forebrain of a cichlid fish, *Astatotilapia burtoni*. J Chem Neuroanat 47:106–115.

Okazaki H, Lipkin LE, Aronson SM. 1961. Diffuse intracytoplasmatic ganglionic inclusions (Lewy type) associated with progressive dementia and quadriparesis in flection. J Neuropathol Exp Neurol 20:237–244.

Panula P, Chen YC, Priyadarshini M, Kudo H, Semenova S, Sundvik M, Sallinen V. 2010. The comparative neuroanatomy and neurochemistry of zebrafish CNS systems of relevance to human neuropsychiatric diseases. Neurobiol Dis 40:46–57.

Pérez SE, Yáñez J, Marín O, Anadón R, González A, Rodríguez-Moldes I. 2000. Distribution of choline acetyltransferase (ChAT) immunoreactivity in the brain of the adult trout and tract-tracing observations on the connections of the nuclei of the isthmus. J Comp Neurol 428: 450–474.

Perez RG, Waymire JC, Lin E, Liu JJ, Guo F, Zigmond MJ. 2002. A role for α-synuclein in the regulation of dopamine biosynthesis. J Neurosci 22:3090–3099.

Phillips W, Michell A, Pruess H, Barker RA. 2009. Animal models of neurodegenerative diseases. Methods Mol Bio 549:137–155.

Rink E, Wullimann MF. 2001. The teleostean (zebrafish) dopaminergic system ascending to the subpallium (striatum) is located in the basal diencephalon (posterior tuberculum). Brain Res 889:316–330.

Rink E, Wullimann MF. 2002. Connections of the ventral telencephalon and tyrosine hydroxylase distribution in the zebrafish brain (*Danio rerio*) lead to identification of an ascending dopaminergic system in a teleost. Brain Res Bull 57:385–387.

Rink E, Wullimann MF. 2004. Connections of the ventral telencephalon (subpallium) in the zebrafish (*Danio rerio*). Brain Res 1011:206–220.

Robertson DC, Schmidt O, Ninkina N, Jones PA, Sharkey J, Buchman VL. 2004. Developmental loss and resistance to MPTP toxicity of dopaminergic neurons in substantia nigra pars compacta of γ-synuclein, α-synuclein and double α/γ-synuclein null mutant mice. J Neurochem 89: 1126–1136.

Rodriguez-Moldes I, Molist P, Adrio F, Pombal MA, Yanez SE, Mandado M, Marin O, Lopez JM, Gonzales A, Anadon R. 2002. Organization of cholinergic systems in the brain of different fish groups: a comparative analysis. Brain Res Bull 57:331–334.

Sager JJ, Bai Q, Burton EA. 2010. Transgenic zebrafish models of neurodegenerative diseases. Brain Struct Funct 214: 285–302.

Scholz SW, Houlden H, Schulte C, Sharma M, Li A, Berg D, Melchers A, Paudel R, Gibbs R, Simon-Sanchez J, Paisan-Ruiz C, Bras J, Ding J, Chen H, Traynor BJ, Arepalli S, Zonozi RR, Revesz T, Holton J, Wood N, Lees A, Oertel W, Wullner U, Goldwurm S, Pellecchia MT, Illing T, Riess O, Fernandez HH, Rodriguez RL, Okun MS, Poewe W, Wenning GK, Hardy JA, Singleton AB, Gasser T. 2009. SNCA variants are associated with increased risk for multiple system atrophy. Ann Neurol 65:610–614.

Sharma N, Hewlett J, Ozelius LJ, Ramesh V, McLean PJ, Breakefield XO, Hyman BT. 2001. A close association of torsinA and alpha-synuclein in Lewy bodies: a fluorescence resonance energy transfer study. Am J Pathol 159: 339–344.

Spillantini MG, Schmidt ML, Lee VM, Trojanowski JQ, Jakes R, Goedert M. 1997. Alpha-synuclein in Lewy bodies. Nature 388:839–840.

Sun Z, Gitler AD. 2008. Discovery and characterization of three novel synuclein genes in zebrafish. Dev Dyn 237: 2490–2495.

Tiunova AA, Anokhin KV, Saha AR, Schmidt O, Hanger DP, Anderton BH, Davies AM, Ninkina NN, Buchman VL. 2000. Chicken synucleins: cloning and expression in the developing embryo. Mech Dev 99:195–198.

Totterdel S, Hanger D, Meredith GE. 2004. The ultrastructural distribution of alpha-synuclein-like protein in normal mouse brain. Brain Res 1004:61–72.

Ubeda-Banon I, Saiz-Sanchez D, de la Rosa-Prieto C, Argandona-palacios L, Garcia-Munozguren S, Martinez-Marcos A. 2010. α-Synucleinopathy in the human olfactory system in Parkinson's disease: involvement of calcium-binding protein- and substance P-positive cells. Acta Neuropathol 119:723–735.

Vilar M, Chou HT, Luhrs T, Maji SK, Riek-Loher D, Verel R, Manning G, Stahlberg H, Riek R. 2008. The fold of α-synuclein fibrils. Proc Natl Acad Sci U S A 105:8637–8642.

Vivacqua G, Yin JJ, Casini A, Li X, Li YH, D'Este L, Chan P, Renda TG, Yu S. 2009. Immunolocalization of alpha-synuclein in the rat spinal cord by two novel monoclonal antibodies. Neuroscience 158:1478–1487.

Vivacqua G, Casini A, Vaccaro R, Fornai F, Yu S, D'Este L. 2011a. Different sub-cellular localization of alpha-synuclein in the C57/BL\6J mouse's central nervous system by two novel monoclonal antibodies. J Chem Neuroanat 41:97–110.

Vivacqua G, Casini A, Vaccaro R, Parisi Salvi E, Pasquali L, Fornai F, Yu S, D'Este L. 2011b. Spinal cord and parkinsonism: neuromorphological evidences in humans and experimental studies. J Chem Neuroanat 42:327–340.

Volles MJ, Lansbury PT Jr. 2007. Relationships between the sequence of alpha-synuclein and its membrane affinity, fibrillization propensity, and yeast toxicity. J Mol Biol 366:1520–1522.

Willemsen R, Hasselaar W, van der Linde H, Bonifati V. 2008. Zebrafish as a new model organism for Parkinson's disease. In: Proceedings of Measuring Behavior, Maastrict, The Netherlands: August 26–29, 2008, p 50–51. Spink AJ, Ballintijn MR, Bogers ND, Grieco F, Loijens LWS, Noldus LPJJ, Smit G, Zimmerman PH.

Wullimann MF, Rupp B, Reichert H, editors. Neuroanatomy of the zebrafish brain: a topological atlas. Basel, Boston, Berlin: Birkhäuser, 1996.

Wulliman MF. 1997. The central nervous system. In: Evans DH, editor. The physiology of fishes. New York: CRC Press. p 245–282.

Yamada M, Iwatsubo T, Mizuno Y, Mochizuki H. 2004. Overexpression of alpha-synuclein in rat substantia nigra results in loss of dopaminergic neurons, phosphorilation of alpha-synuclein and activation of caspase-9: resemblance to pathogenetic changes in Parkinson's disease. J Neurochem 91:451–461.

Yamamoto N, Ito H. 2005a. Fiber connections of the central nucleus of semicircular torus in cyprinids. J Comp Neurol 491:186–211.

Yamamoto N, Ito H. 2005b. Fiber connections of the anterior preglomerular nucleus in cyprinids with notes on telencephalic connections of the preglomerular complex. J Comp Neurol 491:212–233.

Yamamoto N, Ito H. 2008. Visual, lateral line, and auditory ascending pathways to the dorsal telencephalic area through the rostrolateral region of the lateral preglomerular nucleus in cyprinids. J Comp Neurol 508:615–647.

Yamamoto K, Ruuskanen JO, Wullimann MF, Vernier P. 2011. Differential expression of dopaminergic cell markers in the adult zebrafish forebrain. J Comp Neurol 519:576–598.

Yang ML, Hasadsri L, Woods WS, George JM. 2010. Dynamic transport and localization of alpha-synuclein in primary hippocampal neurons. Mol Neurodegener 5:9.

Yoshida H, Craxton M, Jakes R, Zibaee S, Tavaré R, Fraser G, Serpell LC, Davletov B, Crowther RA, Goedert M. 2006. Synuclein proteins of the puffer fish *Fugu rubripes*: sequences and functional characterization. Biochemistry 45:2599–2607.

Yu S, Ueda K, Chan P. 2005. Alpha-synuclein and dopamine metabolism. Mol Neurobiol 31:243–254.

Yu S, Li X, Liu G, Han J, Zhang C, Li Y, Xu S, Liu C, Gao Y, Yang H, Uèda K, Chan P. 2007. Extensive nuclear localization of alpha-synuclein in normal rat brain neurons revealed by a novel monoclonal antibody. Neuroscience 145:539–555.

Zhang L, Zhang C, Zhu Y, Cai Q, Chan P, Ueda K, Yu S, Yang H. 2008. Semi-quantitative analysis of alpha-synuclein in subcellular pools of rat brain neurons: an immunogold electron microscopic study using a C-terminal specific monoclonal antibody. Brain Res 1244:40–52.